



NATIONAL TECHNICAL UNIVERSITY OF ATHENS
SCHOOL OF MECHANICAL ENGINEERING
DEPT. OF MECHANICAL DESIGN & AUTOMATIC CONTROL

Collaborative Object Transportation Under Planar Motion Constraint

Diploma Thesis

PARASKEVAS C. THEOLOGITIS

Advisor

Kostas J. Kyriakopoulos, Professor NTUA

Athens, February 2022

– this page is intentionally left blank –

Declaration of responsibility for plagiarism and theft of intellectual property:

I have read and understood the rules on plagiarism and how to properly cite sources contained in the Guide to Writing Dissertations. I declare that, to the best of my knowledge, the content of this Thesis is the product of my own work and there are references to all the sources I have used.

The opinions and conclusions contained in this Diploma Thesis are those of the author and should not be interpreted as representing the official positions of the School of Mechanical Engineering or the National Technical University of Athens.

Paraskevas C. Theologitis

Acknowledgements

I am grateful to all the people that supported me throughout my undergraduate studies in National Technical University of Athens that are culminated by writing of the present thesis.

I would like to thank Professor K.J. Kyriakopoulos and C.P. Bechlioulis for entrusting me with the project and for the guidance and support during its preparation. They have been a source of inspiration regarding my research interests.

In addition, I am extremely thankful to my friends and family that supported me in multiple ways. Besides my mother and brothers, I would like to pay a special tribute to my grandmother and express my true gratitude for her presence in my life. For this reason, together with her recent passing, I dedicate the present work to her, along with the pledge that there will be more to come.



NATIONAL TECHNICAL UNIVERSITY OF ATHENS
SCHOOL OF MECHANICAL ENGINEERING
DEPT. OF MECHANICAL DESIGN & AUTOMATIC CONTROL

Collaborative Object Transportation Under Planar Motion Constraint

Diploma Thesis

PARASKEVAS C. THEOLOGITIS

Advisor

Kostas J. Kyriakopoulos, Professor NTUA

Athens, February 2022

Abstract

One of the pinnacles of human progress is, without a doubt, the automation technology that was developed in the past century. The advancements towards new directions and uses regarding this technology have been manifested as the development of software, in order to make the robots smarter, granting human-like characteristics, for the purpose of collaborating with other agents. As it is often the case, the collaboration is sought out on the basis of handling difficult tasks that the employment of a robotic helper would render safer and easier. Under this prism, Mobile Manipulators or Mobile Robots provide the needed mobility in order to act in the same physical domain as a human and thus efficiently collaborate, if needed, in industrial or other spaces.

In this direction, and in the spirit of assisting such research, a configurable model of a system with multiple Mobile Operators cooperatively transporting an object is developed. Besides the dynamic modelling of the robots and the object itself, an important aspect, in the context of simulation, lies in the calculation of the interaction between said sub-systems. This work constitutes a basic model able to be utilised in a number of cases.

For example it can be utilised for carrying out simulations of autonomous vehicles performing a prescribed task, such as transporting an object, where navigation and collision-avoidance schemes are present. Also, in the case of human-robot collaboration where an added effect, that of the human on the object, must be considered and interpreted by an algorithm in order to efficiently assist the human in performing a task.



ΕΘΝΙΚΟ ΜΕΤΣΟΒΙΟ ΠΟΛΥΤΕΧΝΕΙΟ
ΣΧΟΛΗ ΜΗΧΑΝΟΛΟΓΩΝ ΜΗΧΑΝΙΚΩΝ
ΤΟΜΕΑΣ ΜΗΧ. ΚΑΤΑΣΚΕΥΩΝ ΚΑΙ ΑΥΤΟΜΑΤΟΥ ΕΛΕΓΧΟΥ

Συνεργατική Μεταφορά Αντικειμένου που Υπόκειται σε Κινηματικούς Περιορισμούς επί Επιπέδου

Διπλωματική Εργασία
ΠΑΡΑΣΚΕΥΑΣ Χ. ΘΕΟΛΟΓΙΤΗΣ

Επιβλέπων
Κώστας Ι. Κυριακόπουλος, Καθηγητής ΕΜΠ

Αθήνα, Φεβρουάριος 2022

Abstract

Μια από τις κορυφές της ανθρώπινης προόδου είναι σίγουρα η τεχνολογία αυτοματισμού που αναπτύχθηκε τον περασμένο αιώνα. Η πρόοδος προς νέες κατευθύνσεις και χρήσεις, όσον αφορά την τεχνολογία, σχετίζεται με την ανάπτυξη λογισμικού, προκειμένου τα ρομπότ να γίνουν πιο έξυπνα, προσδίδοντας χαρακτηριστικά που μοιάζουν με του ανθρώπου, με σκοπό τη συνεργασία με άλλους παράγοντες. Όπως συμβαίνει συχνά, η συνεργασία υλοποιείται στο πλαίσιο του χειρισμού δύσκολων εργασιών που η χρήση ενός ρομπότ θα καθιστούσε ασφαλέστερη και ευκολότερη. Υπό αυτό το πρίσμα, οι κινητοί χειριστές ή τα κινητά ρομπότ παρέχουν την απαραίτητη κινητικότητα προκειμένου να δρουν στον ίδιο φυσικό χώρο με τον άνθρωπο και να συνεργάζονται αποτελεσματικά, αν χρειαστεί, σε βιομηχανικούς ή άλλους χώρους.

Προς αυτή την κατεύθυνση, και στο πνεύμα της υποβοήθησης μιας τέτοιας έρευνας, αναπτύσσεται ένα παραμετροποιήσιμο μοντέλο ενός συστήματος με πολλούς Κινητούς Χειριστές που μεταφέρουν συνεργατικά ένα αντικείμενο. Εκτός από τη δυναμική μοντελοποίηση των ρομπότ και του ίδιου του αντικειμένου, μια σημαντική πτυχή, στο πλαίσιο της προσομοίωσης, έγκειται στον υπολογισμό της αλληλεπίδρασης μεταξύ των εν λόγω υποσυστημάτων. Η εργασία αυτή αποτελεί ένα βασικό μοντέλο που μπορεί να χρησιμοποιηθεί σε διάφορες περιπτώσεις.

Για παράδειγμα, μπορεί να χρησιμοποιηθεί για την προσομοίωση αυτόνομων οχημάτων που εκτελούν ένα προκαθορισμένο έργο, όπως η μεταφορά ενός αντικειμένου, όπου υπάρχουν συστήματα πλοήγησης και αποφυγής συγκρούσεων. Επίσης, στην περίπτωση συνεργασίας ανθρώπου-ρομπότ, όπου πρέπει να ληφθεί υπόψη και να ερμηνευθεί από έναν αλγόριθμο μια πρόσθετη επίδραση, αυτή του ανθρώπου στο αντικείμενο, προκειμένου να βοηθηθεί αποτελεσματικά ο άνθρωπος στην εκτέλεση μιας εργασίας.

List of Abbreviations

AI Artificial Intelligence

DH Denavit-Hartenberg

DoF Degree of Freedom

EE End Effector

IR Infrared

MIC Multiple Impedance Control

MM Mobile Manipulator

OIC Object Impedance Control

pHRI physical Human-Robot Interaction

Contents

1	Introduction	1
2	Technical Problem Statement	3
3	Mobile Manipulator Modelling	4
3.1	Forward Kinematics	4
3.1.1	Vehicle Kinematics	4
3.1.2	Manipulator Kinematics	5
3.1.3	Mobile Manipulator Kinematics	6
3.2	Differential Kinematics	7
3.2.1	Manipulator Differential Kinematics	7
3.2.2	Mobile Manipulator Differential Kinematics	8
3.2.3	Alternative method	9
3.3	Dynamics	11
3.3.1	Vehicle Dynamics	11
3.3.2	Manipulator Dynamics	13
3.3.3	Interaction Dynamics	14
3.3.4	Mobile Manipulator Dynamics	15
3.4	Dynamics in Task Space	17
3.4.1	Non Redundant Systems	17
3.4.2	Redundant Systems	18
4	Object Modelling and Grasping	20
5	Interaction Wrench	23
5.1	Constraint equation	23
5.2	Case of a single manipulator	24
5.3	Case of multiple manipulators	26
6	Control Scheme	27
7	Simulation and Results	29
7.1	Software	29
7.2	Results	29
8	Conclusion	33
	Εκτενής Περίληψη Διπλωματικής Εργασίας	34
	Μοντελοποίηση Κινητού Χειριστή	34
	Κινηματική	34
	Διαφορική Κινηματική	35
	Δυναμική	37
	Μοντελοποίηση Αντικειμένου	42
	Υπολογισμός Δυναμο-Ροπής Αλληλεπίδρασης	44
	Σχήμα Ελέγχου	46
	Προσομοίωση και Αποτελέσματα	47

Bibliography

52

Appendix A Software Structure

i

Scripts	i
MobManModel.m	i
ObjAndGrasp.m	i
Constraint.m	i
IniConCalc.m	i
ControlAndFrictionParams.m	ii
Functions	ii
PseudoInertia.m	ii
ManKin.m	ii
ManJac.m	ii
MManJac.m	ii
ManDyn.m	ii
IntDyn.m	iii
SkewSM.m	iii
GraspMatrix.m	iii

– this page is intentionally left blank –

1 Introduction

The notion of automation dates back thousands of years. Typical examples are inventions of Hero of Alexandria, such as the famous temple gate opening system, and the anti-kythera mechanism. Romans also came up with contraptions that utilized some form of automatic action, albeit as mere entertainment tools. Coupling automation with the human form resulted in the presentation of the Mechanical Knight by Leonardo da Vinci. Although these ideas existed for many centuries it was not until the advent of electronics in the 20th century that building and controlling elaborate automation constructions was made possible. One can think of 1921, the year the term 'robot' was coined, as the beginning of the technology as we know it today. At first, the idea of humanoids excited researchers and public, although with no capability of performing complex task, owing to the infancy of the technology. After World War II and the technological leaps that the war effort brought, especially regarding digital computers, led robotics to a similar path. As a milestone, in 1961 the first industrial robot was installed [1]. After that the field of robotics has been continuously and rapidly evolving during the decades that followed.

Initially used for industry, robots were programmed to perform repetitive tasks that relied only on the kinematic control of the mechanical arm. In order to further enhance the capabilities of these machines, for productive and technological purposes, other systems must be added. Shortly after the advent of commercially available microcomputers, they were used for the realization of real time controllers, exploiting the fast calculation capabilities, such as in [2]. Other additions included computer vision [3], [4], sonar, laser or Infrared (IR) sensors for identifying the environment and working within its limits [5–7] and later further developments [8]. These sensors provided robots with a way to interpret the environment and are, still, widely used, while constantly evolving in terms of hardware, such as LiDAR, and software, such as SLAM [9]. In turn, the development of mobile robots flourished, owing to the ability to work in the same physical domain as humans. Various types of mobile robots exist, mainly wheeled and legged robots, along with aerial and underwater agents, each designed for a particular technological niche. Besides these, it was of great concern to be able to regulate the interaction force of the robots with the environment, which was achieved through the inclusion of force sensors [10]. Another useful characteristic is the intelligence, that can be achieved through the use of AI [11–14]. Cutting edge technology that is currently researched, includes object transportation [15], [16] or picking up produce from a field [17] or in space [18]. Aerial vehicles can be utilised for deliveries that time is critical (e.g. pharmaceuticals) and navigating and performing surveys in difficult to reach spaces [19]. Similarly, underwater vehicles can be used for inspections that would otherwise be dangerous or difficult for humans to perform.

Mobile robots equipped with wheels perform best on smooth surfaces. Thus making this type of robot the obvious choice for use in industrial sites where such surfaces exist. Nonetheless, the advancements of robots in both industry and everyday life proves to be an emerging field that aims to combine the human cognitive skills with the robot capabilities [15]. An area of interest is collaborative transportation

of heavy, bulky objects or supporting of a task performed by a human as a means of increasing its accuracy, e.g. welding. An important aspect of this application is the load which the human and the robot take on and the physical Human-Robot Interaction (pHRI) in general, such as in [23], [16]. Another task this type of robots can perform consists of autonomously working in teams, that is with no human interference, largely inspired by nature such as the works in [20–22].

2 Technical Problem Statement

In order to test out new algorithms, such as control and collaboration schemes or Artificial Intelligence (AI) capabilities for mobile robots, it is mandatory for a model of the physical system to be available. As it is often the case, the physical system is not available; as it happens during designing of a new product. Therefore, to accommodate rapid assessment of the proposed algorithms it is critical that the model of the robot is promptly obtainable. This leads to the need of a parametric model that can be used in a number of cases and for a number of robots. In addition, the calculation of the interaction wrench between each robot and the object must be included as part of the system dynamics.

Regarding the structure of this thesis it is organised as follows. First, in section 3 and 4, the modelling of a MM and of the object are provided. In section 5, the reduction of the algebraic-differential system for multiple MMs is presented. In section 6, a control scheme is proposed, base on the notion of (multiple) impedance control. In section 7, the simulation results are presented and reviewed. Finally, section 8 concludes the thesis.

3 Mobile Manipulator Modelling

Mathematical modelling of a Mobile Manipulator (MM) can be challenging, especially with MMs that are equipped with a high number of Degree of Freedom (DoF) manipulator. Therefore we choose a modular approach that will allow for the analysis of the wheeled platform and n_r -DoF manipulator to be carried out separately. In that way, the typical modelling of manipulators and a plethora of platform models from the bibliography can be utilized. Then, by considering the dynamic interactions due to the coupling of the two subsystems and adding the corresponding terms in the separate dynamic equations will yield the system of the total (coupled) dynamics of the MM. It is also noted, that the interaction dynamics can be further studied, by study of the respective matrices, if a more detailed analysis is needed.

3.1 Forward Kinematics

Forward kinematics usually describe the End Effector (EE) *pose* (position and orientation) with respect to the base of the manipulator. In the MM case the base of the manipulator is rigidly attached to the platform. In light of this, we need to define multiple frames as follows:

- the world (inertial) frame $\{W\}$
- the vehicle (platform) frame $\{V\}$, attached on the centroid of the platform and
- the frames sequence from $\{0\}$ or $\{M\}$ frame to $\{n\}$ or $\{E\}$ frame, attached on the joints of the manipulator following standard DH notation.

3.1.1 Vehicle Kinematics

The vehicle frame is moving and rotating with respect to the world frame, essentially expressing the planar movement of the platform. On that note, the vector of platform variables are defined as $\mathbf{q}_v = [q_{v,1} \ q_{v,2} \ \dots \ q_{v,n}]^T$. In this case, a 3-DoF (planar) vehicle is considered where $\mathbf{q}_v = [x_v \ y_v \ \phi]^T$. Thus, a proper homogeneous transformation matrix that relates the aforementioned frames is defined

$${}^W\mathbf{T}_V = {}^W\mathbf{T}_V(\mathbf{q}_v) = \begin{bmatrix} \mathbf{R}_V & \mathbf{r}_v \\ \mathbf{0}_{1 \times 3} & 1 \end{bmatrix} \quad (3.1)$$

The transformation consists of a rotation, ϕ , about the Z-axis

$$\mathbf{R}_V = \mathbf{R}_V(\phi) = \begin{bmatrix} \cos \phi & -\sin \phi & 0 \\ \sin \phi & \cos \phi & 0 \\ 0 & 0 & 1 \end{bmatrix} \quad (3.2)$$

and a translation expressed by vector $\mathbf{r}_v = [x_v \ y_v \ z_v]^T$, which describes the coordinate of the vehicle's Center of Mass (CoM) expressed in frame $\{W\}$. The

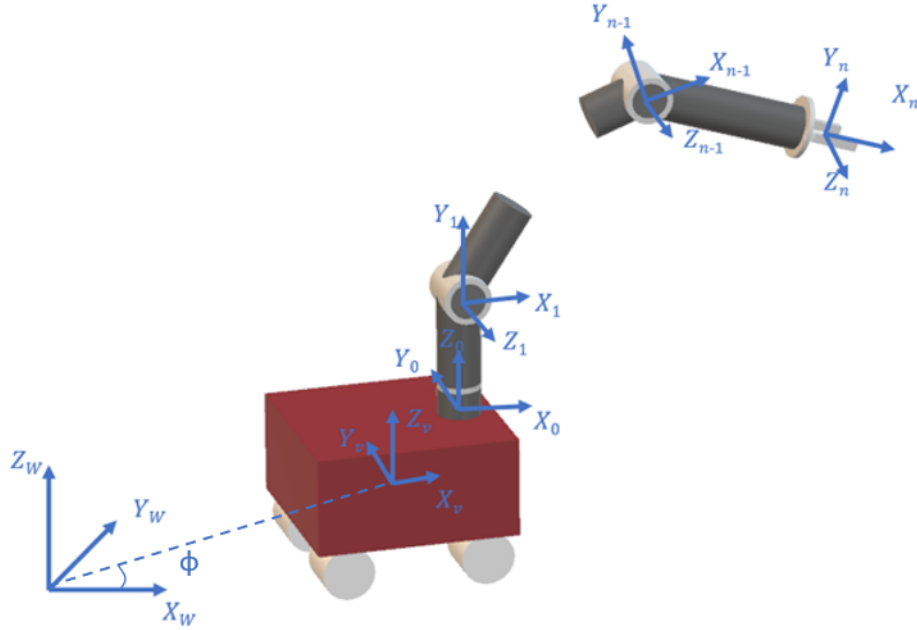


Figure 3.1: Mobile Manipulator with the frames attached

Z coordinate actually is a constant offset of the vehicle frame, accounting for the wheels and overall configuration of the moving platform. Similarly a transformation matrix between the base of the manipulator and the platform can also be defined. This transformation matrix is constant due to the absence of relative motion owing to the rigidity assumption. For simplicity, it was considered that the frames have the same orientation, as seen in figure 3.1.

$${}^V\mathbf{T}_M = \begin{bmatrix} \mathbf{I}_{3 \times 3} & \mathbf{r}_{rp} \\ \mathbf{0}_{1 \times 3} & 1 \end{bmatrix} \quad (3.3)$$

where $\mathbf{I}_{3 \times 3}$ is the unity matrix and $\mathbf{r}_{rp} = [x_{rp} \ y_{rp} \ z_{rp}]^T$ is the position vector from the CoM of the platform to the base of the manipulator expressed in frame $\{V\}$, that is the mount position of the manipulator.

3.1.2 Manipulator Kinematics

The standard Denavit-Hartenberg convention will be used for the kinematics of the (open-chain) manipulator. Also, defining the manipulator variables vector $\mathbf{q}_r = [q_{r,1} \ q_{r,2} \ \dots \ q_{r,n}]^T$, where n_r is the number of DoFs of the manipulator. The frame $\{0\}$ is arbitrary placed and is commonly placed on the base of the manipulator, frame $\{1\}$ is placed on the first joint and so on, while frame $\{n\}$ is placed on the End Effector (EE) of the robot. The transformation between two successive

frames is given by:

$${}^{i-1}\mathbf{T}_i = \begin{bmatrix} \cos \theta_i & -\cos \alpha_i \sin \theta_i & \sin \alpha_i \sin \theta_i & a_i \cos \theta_i \\ \sin \theta_i & \cos \alpha_i \cos \theta_i & -\sin \alpha_i \cos \theta_i & a_i \sin \theta_i \\ 0 & \sin \alpha_i & \cos \alpha_i & d_i \\ 0 & 0 & 0 & 1 \end{bmatrix} \quad (3.4)$$

The four parameters a_i , α_i , d_i , θ_i , usually presented in the form of a table describe

Link i	a_i	α_i	d_i	θ_i
1				
2				
\vdots				
n_r				

Table 3.1: Denavit-Hartenberg parameter table

two translations and two rotations between successive frames. The manipulator variables vector \mathbf{q}_r consists of either θ_i or d_i depending on whether the i -th joint is *revolute* or *prismatic*, respectively, while the other two parameters are constant. At last, the transformation matrix relating the base frame to the EE frame is given by

$${}^M\mathbf{T}_e = {}^M\mathbf{T}_e(\mathbf{q}_r) = {}^0\mathbf{T}_n = {}^0\mathbf{T}_1 \cdot {}^1\mathbf{T}_2 \cdot \dots \cdot {}^{n-1}\mathbf{T}_n \quad (3.5)$$

3.1.3 Mobile Manipulator Kinematics

At last, the total transformation matrix relating the inertial frame to the End Effector frame is given by:

$${}^W\mathbf{T}_e = {}^W\mathbf{T}_V \cdot {}^V\mathbf{T}_M \cdot {}^M\mathbf{T}_e \quad (3.6)$$

Equation 3.6 along with the equations 3.1-3.5 constitute the kinematic model of the MM. Forward kinematics, as stated above, consist of the position and orientation of the EE which are expressed by the first three elements of the fourth column and the 3x3 rotation sub-matrix

$${}^W\mathbf{T}_e = {}^W\mathbf{T}_e(\mathbf{q}) = \begin{bmatrix} \mathbf{R}_e & \mathbf{p}_e \\ \mathbf{0}_{1 \times 3} & 1 \end{bmatrix} \quad (3.7)$$

where, in general, the homogeneous transformation from the world frame to the EE frame of the MM is a function of its variables, \mathbf{q} , defined as

$$\mathbf{q} = \begin{bmatrix} \mathbf{q}_v \\ \mathbf{q}_r \end{bmatrix} \quad (3.8)$$

3.2 Differential Kinematics

Differential kinematics, expressed through the Jacobian, are a description of the relationship between joint velocities, $\dot{\mathbf{q}}$, and End Effector velocities, $\dot{\mathbf{x}}_e$. The usual case involves a fixed-base manipulator where its Jacobian calculation is a straightforward task involving the manipulator kinematics of the previous section [24]. Therefore, to enable modelling different manipulators with different mounting options to be faster and easier, it is of interest to express the Jacobian of the MM, \mathbf{J} , through the respective manipulator's fixed-base Jacobian, \mathbf{J}_{FB} . In order to achieve this, first the system kinematics must be described and, afterwards, through proper manipulation of the expression, the fixed-base Jacobian is ought to arise [25]. In the following, the equations will use the convention that an left superscript means "expressed in frame" and a right superscript means "with respect to" while a right subscript means "of the" and "of the frame" for lower-case and upper-case index respectively. Lastly, a missing left superscript denotes that the vector is expressed in the world frame, $\{W\}$.

3.2.1 Manipulator Differential Kinematics

Let us define the relationship involving the fixed base Jacobian, that is the End Effector velocities are expressed with respect to the base of the manipulator as follows

$${}^V \dot{\mathbf{x}}_e^M = \begin{bmatrix} {}^V \dot{\mathbf{p}}_e^M \\ {}^V \dot{\boldsymbol{\omega}}_e^M \end{bmatrix} = \mathbf{J}_{FB} \dot{\mathbf{q}}_r \quad (3.9)$$

where $\dot{\mathbf{q}}_r$ denote the variable states of the manipulator. Notice that the usual notation has been modified in order to accommodate for the convention mentioned in the start of the chapter. Furthermore, the Jacobian in general can be compartmentalized

$$\mathbf{J}_{FB} = \begin{bmatrix} \mathbf{J}_P \\ \mathbf{J}_O \end{bmatrix} \quad (3.10)$$

where the P and O subscripts refer to the linear and angular contribution of the joint velocities, respectively. By differentiating the kinematics described by equation 3.5 and by substituting the derivative of a rotation matrix the velocity composition rule arises. Eventually, if the fixed-base Jacobian consists of n columns of the form described in 3.10, then each column can be calculated as

$$\begin{bmatrix} \mathbf{J}_{Pi} \\ \mathbf{J}_{Oi} \end{bmatrix} = \begin{cases} \begin{bmatrix} \mathbf{z}_{i-1} \\ \mathbf{0} \end{bmatrix} & \text{for a } \textit{prismatic} \text{ joint} \\ \begin{bmatrix} \mathbf{z}_{i-1} \times (\mathbf{p}_e - \mathbf{p}_{i-1}) \\ \mathbf{z}_{i-1} \end{bmatrix} & \text{for a } \textit{revolute} \text{ joint} \end{cases} \quad (3.11)$$

where \mathbf{z}_{i-1} , \mathbf{p}_{i-1} are given by the first three elements of the third and fourth column of the transformation matrix from the base of the manipulator to the $\{i-1\}$ frame, respectively, while, \mathbf{p}_e is the position of the EE and is calculated analogous to \mathbf{p}_{i-1} , with the difference that all the manipulator frames are considered. The aforementioned matrices refer to the serial multiplication of all or some of the matrices described by equation 3.4.

3.2.2 Mobile Manipulator Differential Kinematics

Based on the system kinematics, one can write [25]:

$$\boldsymbol{\omega}_e = \boldsymbol{\omega}_V + \boldsymbol{\omega}_e^V \quad (3.12)$$

$$\dot{\mathbf{p}}_e = \dot{\mathbf{p}}_V + \boldsymbol{\omega}_V \times \mathbf{p}_e^V + \dot{\mathbf{p}}_e^V \quad (3.13)$$

$$\dot{\mathbf{p}}_e^V = \dot{\mathbf{p}}_e^M + \dot{\mathbf{p}}_M^V \quad (3.14)$$

Since the manipulator is rigidly attached to the platform there is no relative motion between the two and therefore $\dot{\mathbf{r}}_M^V = 0$. Next invoking equations 3.1 and 3.2 we can write

$$\mathbf{p}_e^V = \mathbf{R}_V^V \mathbf{p}_e^V \quad (3.15)$$

$$\dot{\mathbf{p}}_e^M = \mathbf{R}_V^V \dot{\mathbf{p}}_e^M \quad (3.16)$$

$$\boldsymbol{\omega}_e^V = \boldsymbol{\omega}_e^M = \mathbf{R}_V^V \boldsymbol{\omega}_e^M \quad (3.17)$$

By substituting equations 3.15-3.17 to the system of equations 3.12-3.14 we end up with

$$\dot{\mathbf{x}}_e = \begin{bmatrix} \dot{\mathbf{p}}_e \\ \boldsymbol{\omega}_e \end{bmatrix} = \begin{bmatrix} \dot{\mathbf{p}}_V \\ \boldsymbol{\omega}_V \end{bmatrix} + \begin{bmatrix} [\boldsymbol{\omega}_V]_{\times} \mathbf{R}_V^V \mathbf{p}_e^V \\ \boldsymbol{\omega}_e \end{bmatrix} + \begin{bmatrix} \mathbf{R}_V^V \dot{\mathbf{p}}_e^M \\ \mathbf{R}_V^V \boldsymbol{\omega}_e^M \end{bmatrix} \quad (3.18)$$

where $[\cdot]_{\times}$ denotes a skew-symmetric matrix, that for a vector $\mathbf{a} = [a_x \ a_y \ a_z]^T$ is defined as

$$[\mathbf{a}]_{\times} = \begin{bmatrix} 0 & -a_z & a_y \\ a_z & 0 & -a_x \\ -a_y & a_x & 0 \end{bmatrix} \quad (3.19)$$

In that way the outer product can be represented as a matrix product. Next, the outer product property $\mathbf{a} \times \mathbf{b} = -\mathbf{b} \times \mathbf{a}$ is used and also the fact that for an orthonormal transformation, such as the rotation matrices used, the transpose is identical with the inverse. Hence 3.18 can be written as [24]

$$\dot{\mathbf{x}}_e = \begin{bmatrix} \dot{\mathbf{p}}_e \\ \boldsymbol{\omega}_e \end{bmatrix} = \begin{bmatrix} \mathbf{I} & -\mathbf{R}_V^V [\mathbf{p}_e^V]_{\times} \mathbf{R}_V^T \\ \mathbf{0} & \mathbf{I} \end{bmatrix} \begin{bmatrix} \dot{\mathbf{p}}_V \\ \boldsymbol{\omega}_V \end{bmatrix} + \begin{bmatrix} \mathbf{R}_V^V & \mathbf{0} \\ \mathbf{0} & \mathbf{R}_V^V \end{bmatrix} \begin{bmatrix} \mathbf{R}_V^V \dot{\mathbf{p}}_e^M \\ \mathbf{R}_V^V \boldsymbol{\omega}_e^M \end{bmatrix} \quad (3.20)$$

Lastly, 3.20 can be rewritten in the usual form of a Jacobian

$$\dot{\mathbf{x}}_e = \begin{bmatrix} \dot{\mathbf{p}}_e \\ \boldsymbol{\omega}_e \end{bmatrix} = \begin{bmatrix} \mathbf{J}_v & | & \mathbf{J}_r \end{bmatrix} \begin{bmatrix} \dot{\mathbf{q}}_v \\ \dot{\mathbf{q}}_r \end{bmatrix} = \mathbf{J} \dot{\mathbf{q}} \quad (3.21)$$

and, by considering equations 3.9, 3.20 and 3.21, the sub-matrices are given

$$\mathbf{J}_v = \begin{bmatrix} \mathbf{I} & -\mathbf{R}_V^V [\mathbf{p}_e^V]_{\times} \mathbf{R}_V^T \\ \mathbf{0} & \mathbf{I} \end{bmatrix} \quad (3.22)$$

$$\mathbf{J}_r = \begin{bmatrix} \mathbf{R}_V^V & \mathbf{0} \\ \mathbf{0} & \mathbf{R}_V^V \end{bmatrix} \mathbf{J}_{FB} \quad (3.23)$$

3.2.3 Alternative method

The preceding analysis arrives at the Geometric Jacobian of the MM which is, in general, not equal to the Analytical Jacobian. The latter consists of the translational velocities and the derivative of the orientation instead of the angular velocities. Nevertheless, there is an alternative method of calculating the End Effector Geometric Jacobian, through the Analytical Jacobian [24]. First, invoking 3.7, linear velocities-related terms can be calculated by differentiating and applying the chain rule on the coordinate vector of the end-effector

$$\dot{\mathbf{p}}_e = \frac{\partial \mathbf{p}_e}{\partial \mathbf{q}} \dot{\mathbf{q}} \quad (3.24)$$

It is easily understood that a similar process can not be utilised for the angular velocities-related part of the Jacobian. This owes to the way the orientation is conventionally described, that is by a 3x3 matrix. Therefore, in order to calculate the contribution of the angular velocities, a minimal representation must be selected, which will allow expressing the orientation with a vector. The representations commonly used consist of the ZYX (Yaw-Pitch-Roll) and ZYZ Euler angles. The analysis that follows uses the former set of Euler angles. Calculating said angles of orientation is a process called *inverse kinematics* and for ZYX minimal representation it is given as

$$\boldsymbol{\varphi}_e = \begin{bmatrix} \psi_e \\ \theta_e \\ \phi_e \end{bmatrix} = \begin{bmatrix} \text{atan2}(r_{32}, r_{33}) \\ \text{atan2}(-r_{31}, \sqrt{r_{32}^2 + r_{33}^2}) \\ \text{atan2}(r_{21}, r_{11}) \end{bmatrix} \quad (3.25)$$

and $r_{ij}, i, j = 1, 2, 3$ are the elements of the rotation matrix \mathbf{R}_e . Notice that the $\text{atan2}()$ function is used, due to its ability to calculate both the angle and the quadrant which it lies.

The angular velocities are related to the orientation rate of change as

$$\boldsymbol{\omega}_e = \mathbf{T}(\boldsymbol{\varphi}_e) \dot{\boldsymbol{\varphi}}_e \quad (3.26)$$

where the matrix relating the two velocity vectors, for ZYX Euler angles, is [26]

$$\mathbf{T}(\boldsymbol{\varphi}_e) = \begin{bmatrix} \cos \theta_{ze} \cos \theta_{ye} & -\sin \theta_{ze} & 0 \\ \sin \theta_{ze} \cos \theta_{ye} & \cos \theta_{ze} & 0 \\ -\sin \theta_{ye} & 0 & 1 \end{bmatrix} \quad (3.27)$$

For different minimal representations, expressions similar to 3.25 and 3.27 can be formulated. Then, it follows that

$$\dot{\boldsymbol{\varphi}}_e = \frac{\partial \boldsymbol{\varphi}_e}{\partial \mathbf{q}} \dot{\mathbf{q}} \quad (3.28)$$

and the Analytical Jacobian \mathbf{J}_A can be defined analogous to equation 3.10 where the partial derivatives of equations 3.24 and 3.28 describe the linear and angular contributions, respectively. It is clear that, based on 3.26, the Analytical and Geometric

Jacobian can be related

$$\mathbf{J} = \begin{bmatrix} \mathbf{I}_{3 \times 3} & \mathbf{0}_{3 \times 3} \\ \mathbf{0}_{3 \times 3} & \mathbf{T}(\varphi_e) \end{bmatrix} \mathbf{J}_A = \mathbf{T}_A \mathbf{J}_A \quad (3.29)$$

Concluding this section, it is considered appropriate to mention an issue that emerges by the usage of Euler angles. Namely, *representation singularities*. When these arise, the solutions of the *inverse kinematics* are degenerated, thus not allowing the calculation of one orientation angle. In addition, the determinant of matrix $\mathbf{T}(\varphi_e)$ becomes zero and by extension inversion is not possible, indicating a subspace of angular velocities that can not be described by the orientation angle velocities [24]. This can be interpreted as an inadequacy of the representation or a trade-off for expressing orientation, described by a 3x3 matrix, with the minimal number of variables, that is a 3x1 vector. On that note, a representation with no singularities are Quaternions where the orientation is described by four numbers, consisting of a vector and a scalar.

3.3 Dynamics

The dynamics are an integral part of the modelling and describe the motion of the MM. Derivation of the dynamic model allows for the study of the system, simulation of motion and testing control strategies that would otherwise demand that the physical system is available. As with the previous sections, the dynamic model of each sub-system is calculated and then the interaction dynamics, due to the coupling, are separately determined and added appropriately. This allows for an easier repetition of the calculations if needed, e.g. for a different manipulator or platform, and for a better analysis of the dynamic interactions. Usually the dynamics are derived through the Euler-Lagrange formulation as it offers a systematic way of analysis that is valuable when dealing with higher order systems, it provides an analytical form of the dynamics and can accommodate further complexities of the system, such as link deformation, if needed [24].

3.3.1 Vehicle Dynamics

As the Mecanum wheeled platform has gained in popularity over the years due to its holonomic nature, one can find numerous models in the bibliography. Detailed analysis of the mecanum wheel platform utilizing the Lagrange equations of the second kind can be found in references [27,28], while others opt for a more simplistic approach that treat the platform and the wheels as a mass in planar motion [29,30]. The platform is expected to move very slowly, therefore a simple model can be

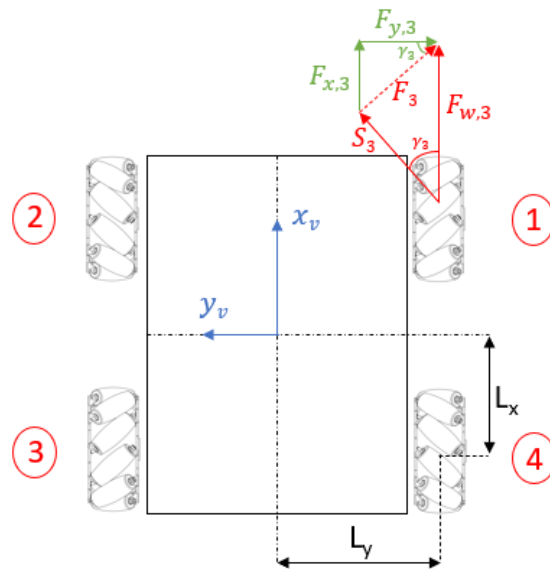


Figure 3.2: Vehicle mounted with 4 Mecanum wheels

utilized, as the omitted dynamics, namely the Coriolis-centrifugal term, is expected to be minuscule. The number of Mecanum wheels that the vehicle is equipped, n_w , is selected to be four, as this is the typical choice. Following a similar derivation as with [30], it is assumed that the platform and wheels form a rigid structure and all the points on the vehicle rotate about the instantaneous rotation centre.

Also, the Mecanum wheels are symmetrically, with respect to the vehicle's CoM (that coincide with its centroid), mounted on the platform. Specifically, the model consists of the inertial forces, the actuation forces and the static friction. Viscous friction is not considered, deemed negligible due to the low speeds that the wheels are expected to rotate.

$$\begin{bmatrix} m_v & 0 & 0 \\ 0 & m_v & 0 \\ 0 & 0 & I_v \end{bmatrix} \begin{bmatrix} \ddot{x}_v \\ \ddot{y}_v \\ \ddot{\phi} \end{bmatrix} = \begin{bmatrix} F_{v,a}^x \\ F_{v,a}^y \\ M_{v,a}^z \end{bmatrix} - \begin{bmatrix} F_s \cdot \text{sgn}(\dot{x}_v) \\ F_s \cdot \text{sgn}(\dot{y}_v) \\ M_s \cdot \text{sgn}(\dot{\phi}) \end{bmatrix} \quad (3.30)$$

where m_v and I_v refer to the total mass and inertia (around its CoM) of the vehicle. The total mass includes the mass of the platform and the mass of the wheels, while the total inertia includes the inertia of the platform and the wheels' around the platform's CoM. The "s" subscript refers to friction forces and torques. It is noted that in order to implement $\text{sgn}()$ during simulation, $\text{tanh}()$ is used instead as it will not cause problems due to the former non-continuous nature. The forces and moment actuating the vehicle are composed from the forces and moments that are produced from each wheel. Then, further analysis, partially shown in figure 3.2, will compute the total force and moment that act on the platform. All Mecanum wheels have the same angle between the rollers and the wheel axis, that for this particular configuration shown in figure 3.2 can be expressed as $\gamma_i = (-1)^i \cdot 45^\circ$. Also all wheels have the same radius, R_w . Suppose that $\tau_{w,i}$ is the input torque, then the input force is $F_{w,i} = \tau_{w,i}/R_w$. This force can be divided to two components, F_i and S_i , in such way that S_i acts transversely to the roller axis. The latter is called ineffective slip force and the former is the effective drive force. Next, F_i can be further analysed to two more components that lie parallel to the vehicle frame

$$\begin{aligned} F_{x,i} &= F_i \sin \gamma_i = F_{w,i} (\sin \gamma_i)^2 \\ F_{y,i} &= F_i \cos \gamma_i = F_{w,i} \cos \gamma_i \sin \gamma_i \end{aligned} \quad (3.31)$$

Similarly, the torque is calculated by accounting for the torque of each force on x and y direction

$$M_{z,i} = L_y F_{x,i} + L_x F_{y,i} \quad (3.32)$$

Concluding the force analysis, the total input vector of the vehicle is calculated as the sum of each wheel contribution and then is transformed to the world frame through a 3x3 rotation matrix, which actually is the one defined in equation 3.2. Therefore we can write

$$\begin{bmatrix} F_{v,a}^x \\ F_{v,a}^y \\ M_{v,a}^z \end{bmatrix} = \sum_{i=1}^4 \begin{bmatrix} \cos \phi & -\sin \phi & 0 \\ \sin \phi & \cos \phi & 0 \\ 0 & 0 & 1 \end{bmatrix} \begin{bmatrix} F_{x,i} \\ F_{y,i} \\ M_{z,i} \end{bmatrix} \quad (3.33)$$

It is deemed appropriate that the actuation vector is expressed as a product of a matrix, \mathbf{E}_v , with the wheel torque vector.

$$\boldsymbol{\tau}_v = \begin{bmatrix} F_{v,a}^x \\ F_{v,a}^y \\ M_{v,a}^z \end{bmatrix} = \frac{1}{R_w} \sum_{i=1}^4 \begin{bmatrix} A \cos \phi - B \sin \phi \\ A \sin \phi + B \cos \phi \\ AL_y + BL_x \end{bmatrix} \tau_{w,i} = \mathbf{E}_v \boldsymbol{\tau}_w \quad (3.34)$$

where $A = (\sin \gamma_i)^2$ and $B = \cos \gamma_i \sin \gamma_i$. It is obvious that the columns of \mathbf{E}_v are given by the vector in the sum term of equation 3.34. Considering that the standard 45° angle is used

$$\mathbf{E}_v = \frac{1}{2R_w} \begin{bmatrix} \cos \phi + \sin \phi & \cos \phi - \sin \phi & \cos \phi + \sin \phi & \cos \phi - \sin \phi \\ \sin \phi - \cos \phi & \sin \phi + \cos \phi & \sin \phi - \cos \phi & \sin \phi + \cos \phi \\ L_y - L_x & L_y + L_x & L_y - L_x & L_y + L_x \end{bmatrix} \quad (3.35)$$

Lastly, equation 3.30 can be written as

$$\mathbf{M}_{v1} \ddot{\mathbf{q}}_v = \mathbf{E}_v \boldsymbol{\tau}_w - \mathbf{D}_v \quad (3.36)$$

where $\mathbf{q}_v = [x_p \ y_p \ \phi]^T$ as defined in the platform kinematics section.

3.3.2 Manipulator Dynamics

As mentioned in the beginning of the dynamics section, the Euler-Lagrange method is usually used for systems with a high number of DoFs. This is accomplished by utilizing the transformation matrices from kinematic analysis [28]. First, let \mathcal{K} and \mathcal{V} be the total kinetic energy and potential energy of the manipulator, respectively. Then, the *Lagrangian* is defined as

$$\mathcal{L}(\mathbf{q}_r, \dot{\mathbf{q}}_r) = \mathcal{K}(\mathbf{q}_r, \dot{\mathbf{q}}_r) - \mathcal{V}(\mathbf{q}_r) \quad (3.37)$$

Then, the equations of motion of the manipulator are obtained by

$$\frac{d}{dt} \frac{\partial \mathcal{L}}{\partial \dot{q}_{r,i}} - \frac{\partial \mathcal{L}}{\partial q_{r,i}} = \tau_{r,i} \quad i = 1, 2, \dots, n_r \quad (3.38)$$

where $\tau_{r,i}$ is the generalised force corresponding to coordinate $q_{r,i}$. The kinetic and potential energy for the i -th link are given by

$$\mathcal{K}_i = \frac{1}{2} \text{trace} \left[\sum_{j=1}^i \sum_{k=1}^i \frac{\partial \mathbf{T}_i}{\partial q_{r,j}} \mathbf{J}_i \frac{\partial \mathbf{T}_i^T}{\partial q_{r,k}} \dot{q}_{r,j} \dot{q}_{r,k} \right] \quad (3.39)$$

$$\mathcal{V}_i = -m_i \mathbf{g}^T \mathbf{T}_i \bar{\mathbf{r}}_i \quad (3.40)$$

where \mathbf{T}_i is defined similar to 3.5 as $\mathbf{T}_i = {}^0\mathbf{T}_1 \cdot {}^1\mathbf{T}_2 \cdot \dots \cdot {}^{i-1}\mathbf{T}_i$. Also, \mathbf{J}_i and m_i are the pseudo-inertia matrix [31] and mass of the link i , respectively, \mathbf{g}^T is the gravitational acceleration vector defined in the manipulator base frame and $\bar{\mathbf{r}}_i$ is the vector pointing from the origin of frame i to the centroid of the link i expressed in frame i .

Then, the total kinetic and potential energy is calculated by summing the energies of each link, given by 3.39 and 3.40. By utilising equations 3.37, 3.38 and properly grouping the resulting terms, the equations of motion of each manipulator link are a second-order differential equation of the form:

$$\sum_{j=1}^{n_r} M_{ij} \ddot{q}_{r,j} + \sum_{j=1}^{n_r} \sum_{k=1}^{n_r} C_{ijk} \dot{q}_{r,j} \dot{q}_{r,k} + G_i = \tau_{r,i} \quad (3.41)$$

where

$$M_{ij} = \sum_{k=\max(i,j)}^{n_r} \text{trace} \left[\frac{\partial \mathbf{T}_k}{\partial q_{r,i}} \mathbf{J}_k \frac{\partial \mathbf{T}_k^T}{\partial q_{r,j}} \right] \quad (3.42)$$

$$C_{ijk} = \sum_{h=\max(i,j,k)}^{n_r} \text{trace} \left[\frac{\partial \mathbf{T}_h}{\partial q_{r,i}} \mathbf{J}_h \frac{\partial^2 \mathbf{T}_h^T}{\partial q_{r,j} \partial q_{r,k}} \right] \quad (3.43)$$

$$G_i = \sum_{k=i}^{n_r} m_k \mathbf{g}^T \frac{\partial \mathbf{T}_k}{\partial q_{r,i}} \bar{\mathbf{r}}_i \quad (3.44)$$

Furthermore, in manipulators, viscous friction in the joints is typically modelled and, thus, is added to the equations. Then 3.41 can be rewritten as

$$\mathbf{M}_{r1}(\mathbf{q}_r) \ddot{\mathbf{q}}_r + \mathbf{C}_{r1}(\mathbf{q}_r, \dot{\mathbf{q}}_r) + \mathbf{G}_r(\mathbf{q}_r) + \mathbf{D}_r \dot{\mathbf{q}}_r = \boldsymbol{\tau}_r \quad (3.45)$$

where $\mathbf{q}_r = [q_{r,1} \ q_{r,2} \ \dots \ q_{r,n}]^T$ and \mathbf{D}_r is a diagonal matrix that its elements are the respective viscous friction coefficients.

3.3.3 Interaction Dynamics

In a similar way, the matrices that describe the interaction dynamics between the platform and the manipulator are calculated. In this case, \mathbf{T}_i is defined similar to 3.6 and analogous to the previous section as

$$\mathbf{T}_i = {}^W \mathbf{T}_V \cdot {}^V \mathbf{T}_M \cdot {}^0 \mathbf{T}_1 \cdot {}^1 \mathbf{T}_2 \cdot \dots \cdot {}^{i-1} \mathbf{T}_i \quad (3.46)$$

First, we examine the additional terms for the manipulator dynamic equations. The Coriolis and centrifugal terms caused by the motion of the platform are

$$\begin{aligned} C_{r2}(i) = & 2 \sum_{j=1}^{n_v} \sum_{k=1}^{n_r} \sum_{h=\max(i,k)}^{n_r} \text{trace} \left[\frac{\partial \mathbf{T}_h}{\partial q_{r,i}} \mathbf{J}_h \frac{\partial^2 \mathbf{T}_h^T}{\partial q_{v,j} \partial q_{r,k}} \right] \dot{q}_{v,j} \dot{q}_{r,k} \\ & + \sum_{j=1}^{n_v} \sum_{k=1}^{n_v} \sum_{h=i}^{n_r} \text{trace} \left[\frac{\partial \mathbf{T}_h}{\partial q_{r,i}} \mathbf{J}_h \frac{\partial^2 \mathbf{T}_h^T}{\partial q_{v,j} \partial q_{v,k}} \right] \dot{q}_{v,j} \dot{q}_{v,k} \end{aligned} \quad (3.47)$$

and the matrix expressing the effect of the vehicle's motion on the manipulator

$$R_r(i, j) = \sum_{k=i}^{n_v} \text{trace} \left[\frac{\partial \mathbf{T}_k}{\partial q_{r,i}} \mathbf{J}_k \frac{\partial \mathbf{T}_k^T}{\partial q_{v,j}} \right] \quad 1 \leq i \leq n_r, \ 1 \leq j \leq n_v \quad (3.48)$$

Similarly, the additional terms for the vehicle are

$$M_{v2}(i, j) = \sum_{k=1}^{n_r} \text{trace} \left[\frac{\partial \mathbf{T}_k}{\partial q_{v,i}} \mathbf{J}_k \frac{\partial \mathbf{T}_k^T}{\partial q_{v,j}} \right] \quad 1 \leq i, j \leq n_v \quad (3.49)$$

$$C_{v2}(i) = 2 \sum_{j=1}^{n_r} \sum_{k=1}^{n_v} \sum_{h=j}^{n_r} \text{trace} \left[\frac{\partial \mathbf{T}_h}{\partial q_{v,i}} \mathbf{J}_h \frac{\partial^2 \mathbf{T}_h^T}{\partial q_{r,j} \partial q_{v,k}} \right] \dot{q}_{r,j} \dot{q}_{v,k} \\ + \sum_{j=1}^{n_r} \sum_{k=1}^{n_r} \sum_{h=\max(j,k)}^{n_r} \text{trace} \left[\frac{\partial \mathbf{T}_h}{\partial q_{v,i}} \mathbf{J}_h \frac{\partial^2 \mathbf{T}_h^T}{\partial q_{r,j} \partial q_{r,k}} \right] \dot{q}_{r,j} \dot{q}_{r,k} \quad (3.50)$$

$$R_v(i, j) = \sum_{k=j}^{n_r} \text{trace} \left[\frac{\partial \mathbf{T}_k}{\partial q_{v,i}} \mathbf{J}_k \frac{\partial \mathbf{T}_k^T}{\partial q_{r,j}} \right] \quad 1 \leq i \leq n_v, 1 \leq j \leq n_v \quad (3.51)$$

On a last note, the matrix \mathbf{R}_v must be the transpose of \mathbf{R}_r because they refer to the interaction forces between the two subsystems, vehicle and manipulator. Due to these forming the "mass" matrix of the system and of course this being a physical system this matrix must be positive definite. This can be confirmed by examining equations 3.48 and 3.51.

3.3.4 Mobile Manipulator Dynamics

Taking into consideration the preceding analysis, that is the derivation of vehicle, manipulator and interactions dynamics, the total dynamic equations of the vehicle are

$$\mathbf{M}_{v1} \ddot{\mathbf{q}}_v + \mathbf{C}_{v1}(\mathbf{q}_v, \dot{\mathbf{q}}_v) + \mathbf{C}_{v2}(\mathbf{q}_v, \mathbf{q}_r, \dot{\mathbf{q}}_v, \dot{\mathbf{q}}_r) = \\ \boldsymbol{\tau}_v - \mathbf{D}_v - \mathbf{M}_{v2}(\mathbf{q}_v, \mathbf{q}_r) \ddot{\mathbf{q}}_v - \mathbf{R}_v(\mathbf{q}_v, \mathbf{q}_r) \ddot{\mathbf{q}}_v \quad (3.52)$$

and of the manipulator are

$$\mathbf{M}_{r1}(\mathbf{q}_r) \ddot{\mathbf{q}}_r + \mathbf{C}_{r1}(\mathbf{q}_r, \dot{\mathbf{q}}_r) + \mathbf{C}_{r2}(\mathbf{q}_r, \dot{\mathbf{q}}_r, \dot{\mathbf{q}}_v) + \mathbf{G}_r(\mathbf{q}_r) + \mathbf{D}_r \dot{\mathbf{q}}_r = \\ \boldsymbol{\tau}_r - \mathbf{R}_r(\mathbf{q}_v, \mathbf{q}_r) \ddot{\mathbf{q}}_v \quad (3.53)$$

In order to compact the above equations, some terms are grouped while the arguments of each matrix are dropped for simplicity. Then the total matrices of the MM are synthesized

$$\begin{bmatrix} \mathbf{M}_v & \mathbf{R}_v \\ \mathbf{R}_r & \mathbf{M}_r \end{bmatrix} \begin{bmatrix} \ddot{\mathbf{q}}_v \\ \ddot{\mathbf{q}}_r \end{bmatrix} + \begin{bmatrix} \mathbf{C}_v \\ \mathbf{C}_r \end{bmatrix} + \begin{bmatrix} \mathbf{0}_{n_v} \\ \mathbf{G}_r \end{bmatrix} + \begin{bmatrix} \mathbf{D}_v \\ \mathbf{D}_r \dot{\mathbf{q}}_r \end{bmatrix} = \begin{bmatrix} \boldsymbol{\tau}_v \\ \boldsymbol{\tau}_r \end{bmatrix} \quad (3.54)$$

where

$$\mathbf{M}_v = \mathbf{M}_{v1} + \mathbf{M}_{v2} \quad (3.55)$$

$$\mathbf{C}_v = \mathbf{C}_{v1} + \mathbf{C}_{v2} \quad (3.56)$$

$$\mathbf{M}_r = \mathbf{M}_{r1} \quad (3.57)$$

$$\mathbf{C}_r = \mathbf{C}_{r1} + \mathbf{C}_{r2} \quad (3.58)$$

and by reminding 3.34 the following relationship holds

$$\begin{bmatrix} \boldsymbol{\tau}_v \\ \boldsymbol{\tau}_r \end{bmatrix} = \begin{bmatrix} \mathbf{E}_v \boldsymbol{\tau}_w \\ \boldsymbol{\tau}_r \end{bmatrix} = \begin{bmatrix} \mathbf{E}_v & \mathbf{0}_{n_v \times n_r} \\ \mathbf{0}_{n_r \times n_w} & \mathbf{I}_{n_r \times n_r} \end{bmatrix} \begin{bmatrix} \boldsymbol{\tau}_w \\ \boldsymbol{\tau}_r \end{bmatrix} \quad (3.59)$$

Equation 3.54 can be further compacted, analogous to the typical form of the dynamic equations, as follows

$$\mathbf{M}\ddot{\mathbf{q}} + \mathbf{C} + \mathbf{G} + \mathbf{D} = \mathbf{E}\boldsymbol{\tau} \quad (3.60)$$

For the sake of completeness the matrices shown in equation 3.60 are presented

$$\begin{aligned} \mathbf{M} &= \begin{bmatrix} \mathbf{M}_v & \mathbf{R}_v \\ \mathbf{R}_r & \mathbf{M}_r \end{bmatrix} \in \mathbb{R}^{n \times n}, & \mathbf{C} &= \begin{bmatrix} \mathbf{C}_v \\ \mathbf{C}_r \end{bmatrix} \in \mathbb{R}^n \\ \mathbf{G} &= \begin{bmatrix} \mathbf{0}_{n_v} \\ \mathbf{G}_r \end{bmatrix} \in \mathbb{R}^n, & \mathbf{D} &= \begin{bmatrix} \mathbf{D}_v \\ \mathbf{D}_r \dot{\mathbf{q}}_r \end{bmatrix} \in \mathbb{R}^n, & \mathbf{E} &= \begin{bmatrix} \mathbf{E}_v & \mathbf{0}_{n_v \times n_r} \\ \mathbf{0}_{n_r \times n_w} & \mathbf{I}_{n_r \times n_r} \end{bmatrix} \in \mathbb{R}^{n \times (n_w + n_r)} \end{aligned} \quad (3.61)$$

and the vectors

$$\mathbf{q} = \begin{bmatrix} \mathbf{q}_v \\ \mathbf{q}_r \end{bmatrix} \in \mathbb{R}^n, \quad \boldsymbol{\tau} = \begin{bmatrix} \boldsymbol{\tau}_w \\ \boldsymbol{\tau}_r \end{bmatrix} \in \mathbb{R}^{n_w + n_r} \quad (3.62)$$

where $n = n_v + n_r$ is the total DoFs of the Mobile Manipulator, n_r refers to the number of DoFs of the attached manipulator, while n_v corresponds to the planar DoFs of the vehicle and n_w to the inputs of the vehicle. Also, it is noted that in the present study, the vehicle is considered to be a planar mechanism, thus restricting the DoFs of the vehicle to $n_v = 3$. This might not always be the case, for example as in reference [25], and that is the reason the combined dynamics are given in general form and dimensions. Also from this point forward, $\mathbf{0}$ and \mathbf{I} will refer to the zero and unity matrix, respectively, while the size will be subscripted.

Lastly, when the End Effector of the manipulator interacts with the environment, it is subject to forces, $\mathbf{f}_e \in \mathbb{R}^{3 \times 1}$, and torques, $\boldsymbol{\mu}_e \in \mathbb{R}^{3 \times 1}$. These can be expressed by the *wrench* vector, which is compartmentalized as

$$\mathbf{h}_e = \begin{bmatrix} \mathbf{f}_e \\ \boldsymbol{\mu}_e \end{bmatrix} \in \mathbb{R}^{6 \times 1} \quad (3.63)$$

The wrench vector is usually known to the robot through the force/torque (f/t) sensor attached to its end effector. This means that the measurements are expressed with respect to the world frame. Nevertheless, the dynamic equations refer to joint variables and consequently, the wrench must be transformed, or better projected, to the joints. This is accomplished by taking advantage of the known kineto-static duality property [24]. This is incorporated to the dynamic equation 3.60 as

$$\mathbf{M}\ddot{\mathbf{q}} + \mathbf{n} = \mathbf{E}\boldsymbol{\tau} + \mathbf{J}^T \mathbf{h}_e \quad (3.64)$$

where Coriolis-centrifugal, gravity and friction terms are collected for ease of presentation in the next sections $\mathbf{n}(\mathbf{q}, \dot{\mathbf{q}}) = \mathbf{n} = \mathbf{C} + \mathbf{G} + \mathbf{D}$.

3.4 Dynamics in Task Space

Task space refers to the characterization of a system with respect to the task related variables which usually are the position and orientation of the end effector, that is the robot's means of interaction with the environment. In accordance with the previous analysis an expression of the dynamics of the system in task space can be established. The differential kinematics can provide a relationship between the velocities of the spaces of interest, namely joint space and task space. The former is most often the preferred analysis framework due to the typical analysis tools. Due to the task of the robot, that is handling an object, it will be proven useful that the representation of the dynamics of the system in task space is formulated. The dynamics in task space can be described similar to the previous model as

$$\tilde{\mathbf{M}}\dot{\mathbf{v}}_e + \tilde{\mathbf{C}} + \tilde{\mathbf{G}} + \tilde{\mathbf{D}} = \mathbf{u} + \mathbf{h}_e \quad (3.65)$$

or

$$\tilde{\mathbf{M}}\dot{\mathbf{v}}_e + \tilde{\mathbf{n}} = \mathbf{u} + \mathbf{h}_e \quad (3.66)$$

3.4.1 Non Redundant Systems

To determine the matrices corresponding to task space dynamics the Jacobian relation 3.21 is utilized. By differentiating the aforementioned equation

$$\dot{\mathbf{v}}_e = \ddot{\mathbf{x}}_e = \mathbf{J}\dot{\mathbf{q}} + \mathbf{J}\ddot{\mathbf{q}} \quad (3.67)$$

and by substituting it in equation 3.60 and premultiplying with \mathbf{J}^{-T}

$$\mathbf{J}^{-T}\mathbf{M}\mathbf{J}^{-1}\dot{\mathbf{v}}_e - \mathbf{J}^{-T}\mathbf{M}\mathbf{J}^{-1}\dot{\mathbf{J}}\dot{\mathbf{q}} + \mathbf{J}^{-T}\mathbf{C} + \mathbf{J}^{-T}\mathbf{G} + \mathbf{J}^{-T}\mathbf{D} = \mathbf{u} + \mathbf{h}_e \quad (3.68)$$

and by grouping properly the matrices of the dynamic equation in task space can be computed as

$$\tilde{\mathbf{M}} = \mathbf{J}^{-T}\mathbf{M}\mathbf{J}^{-1} \quad (3.69)$$

$$\tilde{\mathbf{C}} = \mathbf{J}^{-T}\mathbf{C} - \mathbf{J}^{-T}\mathbf{M}\mathbf{J}^{-1}\dot{\mathbf{J}}\dot{\mathbf{q}} \quad (3.70)$$

$$\tilde{\mathbf{G}} = \mathbf{J}^{-T}\mathbf{G} \quad (3.71)$$

$$\tilde{\mathbf{D}} = \mathbf{J}^{-T}\mathbf{D} \quad (3.72)$$

where \mathbf{u} is the task space input wrench and $\mathbf{J}^{-T} = (\mathbf{J}^{-1})^T = (\mathbf{J}^T)^{-1}$. It is noted that the generalised torques in joint space and the task space input are connected through the relation

$$\mathbf{E}\boldsymbol{\tau} = \mathbf{J}^T\mathbf{u} \quad (3.73)$$

The analysis is related to non-redundant systems due to the inversion of the supposedly square Jacobian. In this case, the task space coordinates form an alternative representation of the system, that is a different set of generalised variables. Additionally, due to the Geometric Jacobian used, the new variables refer to the angular velocity of the end effector. In many cases the representation is practical to express the orientation and not the angular velocity. Therefore in order to provide a homogeneous analysis, the dynamics are expressed with respect to angular velocities and

if the orientation dynamics expression is needed, this can be computed by examining equation 3.29, i.e. \mathbf{T}_A^{-1} is a Jacobian relating position and orientation derivatives with the position derivative and angular velocity. Then a transformation similar with the one presented by equations 3.65-3.73 can be performed.

3.4.2 Redundant Systems

Nevertheless, MMs such as those studied in this thesis are, usually, redundant with respect to the task space. This means the task space dynamics under-represent the dynamics of the system or that the task space dynamics are a projection of the dynamics of the system [32]. Initially, equation 3.73 becomes incomplete for a redundant system. This happens because there is an infinity of elementary displacements that can exist without altering the pose of the manipulator. With that in mind, there is a null space associated with some inverse of the transposed Jacobian that describes these torques that can be applied but not alter the resulting wrenches on the effector. By accounting for this null space torques the following relationship holds

$$\mathbf{E}\boldsymbol{\tau} = \mathbf{J}^T \mathbf{u} + [\mathbf{I} - \mathbf{J}^T \mathbf{J}^{T\#}] \boldsymbol{\tau}_o \quad (3.74)$$

where $\boldsymbol{\tau}_o$ is an arbitrary generalized joint torque vector, projected in the null space of the transpose generalised inverse $\mathbf{J}^{T\#}$.

For the case of redundant manipulators the derivation task space model follows a similar path, although, with some extra steps in order to account for the non-square form of the Jacobian. This time, to circumvent the need for Jacobian inversion, equation 3.60 is pre multiplied by $\mathbf{J}\mathbf{M}^{-1}$, and equations 3.68, 3.74 are substituted

$$\begin{aligned} \dot{\mathbf{v}}_e - \dot{\mathbf{J}}\dot{\mathbf{q}} + \mathbf{J}\mathbf{M}^{-1}\mathbf{C} + \mathbf{J}\mathbf{M}^{-1}\mathbf{G} + \mathbf{J}\mathbf{M}^{-1}\mathbf{D} = \\ \mathbf{J}\mathbf{M}^{-1}\mathbf{J}^T \mathbf{u} + \mathbf{J}\mathbf{M}^{-1} [\mathbf{I} - \mathbf{J}^T \mathbf{J}^{T\#}] \boldsymbol{\tau}_o + \mathbf{J}\mathbf{M}^{-1}\mathbf{J}^T \mathbf{h}_e \end{aligned} \quad (3.75)$$

Observing the resulting equation, it is obvious that the acceleration, $\dot{\mathbf{v}}_e$ and the forces \mathbf{u} are related through the matrix $\mathbf{J}\mathbf{M}^{-1}\mathbf{J}^T$. Consequently,

$$\tilde{\mathbf{M}} = (\mathbf{J}\mathbf{M}^{-1}\mathbf{J}^T)^{-1} \quad (3.76)$$

Furthermore, the term of the null space in equation 3.75 torques must be equal to zero, that is

$$\begin{aligned} \mathbf{J}\mathbf{M}^{-1} [\mathbf{I} - \mathbf{J}^T \mathbf{J}^{T\#}] = \mathbf{0} \Rightarrow \\ \mathbf{J}\mathbf{M}^{-1} = \mathbf{J}\mathbf{M}^{-1}\mathbf{J}^T \mathbf{J}^{T\#} \\ \bar{\mathbf{J}}^T = \mathbf{J}^{T\#} = \tilde{\mathbf{M}}\mathbf{J}\mathbf{M}^{-1} \end{aligned} \quad (3.77)$$

where $\bar{\mathbf{J}}$ is said to be the *dynamically consistent* generalised inverse [32]. By further examining equation 3.75 the transformation equations are

$$\tilde{\mathbf{M}} = (\mathbf{J}\mathbf{M}^{-1}\mathbf{J}^T)^{-1} \quad (3.78)$$

$$\tilde{\mathbf{C}} = \bar{\mathbf{J}}^T \mathbf{C} - \tilde{\mathbf{M}}\dot{\mathbf{J}}\dot{\mathbf{q}} \quad (3.79)$$

$$\tilde{\mathbf{G}} = \bar{\mathbf{J}}^T \mathbf{G} \quad (3.80)$$

$$\tilde{\mathbf{D}} = \bar{\mathbf{J}}^T \mathbf{D} \quad (3.81)$$

Lastly, in this case too, expressing the derivative of orientation can be performed as described in the previous section.

4 Object Modelling and Grasping

An object model can consist of the inertial, Coriolis-centrifugal, gravitational and external forces. The latter is composed by friction forces and the forces due to the mobile robots interacting with the object. Modelling only the inertia of the object along with external forces, such as in [16], [33] and [34], shows that the inertia has a cardinal role in the behaviour of the grasped object, thus producing a sufficiently accurate model. Nevertheless, other researchers such as in [35] or [15] have opted for a model with all of the forces mentioned in the beginning of the paragraph. It must be noted that in [15] the object dynamics are considered along an arbitrary point and a linear-parametric form is utilized in order to account for the rough knowledge of the object model. In this study, Coriolis terms are of no concern due to the low movement speeds of the object. First, a system of a single MM grasping an object is considered and, afterwards, the model is generalized for N Mobile Manipulators. Grasping of an object is an important aspect of handling the object. However this thesis aims at the dynamic analysis and control of the system and by extension the condition of grasping is not considered, while its rigidity is assumed (i.e. no relative movement between the grippers and the object).

Consider an object in three dimensions. The $\{O\}$ frame is attached in the object's CoM. Vector \mathbf{r}_k points from the origin of object's frame to the point of grasping, expressed in frame $\{O\}$. The screw vector described in the previous section, is expressed with respect to the manipulator and therefore its opposite is experienced by the object. Following the virtual stick convention, as done in [15], [36], the

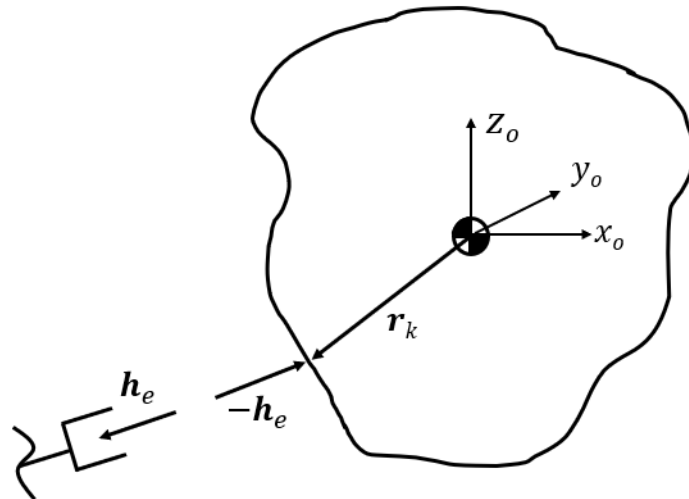


Figure 4.1: Free Body diagram of End Effector and object interaction

k-th EE position and orientation is described through the object's pose. This will prove useful when planning the desired trajectories. In this convention, usually the virtual stick is a vector from the k-th EE to the object's CoM. Instead, the opposite vector is defined, as seen in figure 4.1. The reasoning is that an object-centred definition provides an easier understanding of the *grasp* point, while the

proper transformation is used for the usual virtual stick relation be true. Thus, the kinematics of the virtual stick are

$$\mathbf{p}_k = \mathbf{p}_o + \mathbf{r}_k^o \quad (4.1)$$

$$\mathbf{R}_k = \mathbf{R}_o {}^o\mathbf{R}_k \quad (4.2)$$

where \mathbf{r}_k^o denotes the vector pointing from the object to the EE expressed in world frame and ${}^o\mathbf{R}_k$ refers to the relative orientation between the object and EE frame. Next, the Jacobian of the object and the grasp point is essential for describing the interaction between manipulator and object. The velocity composition rule, based on figure 4.1, gives

$$\mathbf{v}_k = \mathbf{v}_o + \boldsymbol{\omega}_o \times {}^o\mathbf{r}_k^o \quad (4.3)$$

$$\boldsymbol{\omega}_k = \boldsymbol{\omega}_o \quad (4.4)$$

where ${}^o\mathbf{r}_k^o$ is identical to \mathbf{r}_k in figure 4.1. Equations 4.3, 4.4 and can be expressed in a matrix form as

$$\mathbf{v}_k = \mathbf{J}_{ok} \mathbf{v}_o = \begin{bmatrix} \mathbf{I}_{3 \times 3} & -[\mathbf{r}_k]_{\times} \\ \mathbf{0}_{3 \times 3} & \mathbf{I}_{3 \times 3} \end{bmatrix} \mathbf{v}_o \quad (4.5)$$

Lastly, the Jacobian from the EE to the object frame is always full rank due to the rigid grasp assumption. The object's generalised position is defined as

$$\mathbf{x}_o = \begin{bmatrix} \mathbf{p}_o \\ \boldsymbol{\varphi}_o \end{bmatrix} \in \mathbb{R}^{6 \times 1} \quad (4.6)$$

which consists of the object's coordinates and orientation. The orientation can be defined in a number of ways, namely ZYX Euler angles or quaternions are the frequent choices. The generalised velocities are defined as

$$\mathbf{v}_o = \begin{bmatrix} \dot{\mathbf{p}}_o \\ \boldsymbol{\omega}_o \end{bmatrix} \in \mathbb{R}^{6 \times 1} \quad (4.7)$$

Generally, the integral of $\boldsymbol{\omega}_o$ is not the same as the orientation describe by the $\boldsymbol{\varphi}_o$ vector, except of the planar case. Moreover it is supposed to be rigid, therefore the following rigid body dynamics hold

$$\mathbf{M}_o \dot{\mathbf{v}}_o + \mathbf{C}_o(\mathbf{v}_o) \mathbf{v}_o + \mathbf{G}_o + \mathbf{D}_o = \mathbf{h}_o \quad (4.8)$$

where

$$\mathbf{M}_o = \begin{bmatrix} m_o \mathbf{I}_{3 \times 3} & \mathbf{0} \\ \mathbf{0} & \mathbf{I}_o \end{bmatrix} \quad (4.9)$$

$$\mathbf{C}_o = \begin{bmatrix} m_o [\boldsymbol{\omega}_o]_{\times} & \mathbf{0}_{3 \times 3} \\ \mathbf{0}_{3 \times 3} & [\boldsymbol{\omega}_o]_{\times} \mathbf{I}_o \end{bmatrix} \quad (4.10)$$

$$\mathbf{G}_o = \begin{bmatrix} m_o \mathbf{g} \\ \mathbf{0} \end{bmatrix} \quad (4.11)$$

and \mathbf{D}_o contains a friction model of the object motion, m_o is the mass of the object and \mathbf{I}_o is the inertia tensor of the object. The Coriolis matrix, \mathbf{C}_o is given so that the object model and the following derivation are complete. Considering low movement

speed that the object will be moving, only the static friction is considered. Lastly, \mathbf{h}_o denotes the total wrench exerted on the object by the end effector, which in this case

$$\mathbf{h}_o = -\mathbf{G}\mathbf{h}_e \quad (4.12)$$

where $\mathbf{G} = \mathbf{G}_k = \mathbf{J}_{o_k}^T$ is the grasp matrix relating the wrench on the grasp point to the object frame. Also, for presentation homogeneity, consider the object dynamics as

$$\mathbf{M}_o\dot{\mathbf{v}}_o + \mathbf{n}_o = \mathbf{h}_o \quad (4.13)$$

where $\mathbf{n}_o = \mathbf{C}_o\mathbf{v}_o + \mathbf{G}_o + \mathbf{D}_o$. Usually, the object's states include its orientation, as it is a state of interest, and is expressed through a set of Euler angles or quaternions. As mentioned in the previous section regarding transforming the dynamic equations with respect to the orientation variables, similar steps must be taken for the grasp matrix. Specifically, by using equation 3.26 and appropriately modifying the angular-related equations of motion the grasp matrix is then [37]

$$\mathbf{G}_k = \begin{bmatrix} \mathbf{I}_{3 \times 3} & \mathbf{0}_{3 \times 3} \\ \mathbf{T}_A^T [\mathbf{r}_k]_{\times} & \mathbf{T}_A^T \end{bmatrix} \quad (4.14)$$

5 Interaction Wrench

In order to perform a simulation of the dynamical system of one or more MMs grasping an object, it is imperative that the interaction wrench is known. Moreover, control methods that are utilized mandate the knowledge of this wrench, in order to perform the corresponding compensation. In real-time scenarios, where the physical system is available, this wrench is provided by a force/torque sensor attached on (or near) the end effector. To simulate the flow of the f/t sensor readings, a method of calculating the internal wrench in a simulation environment.

The interaction wrench, predominantly results from the apparent rigidity of the grasp. That is, due to the external wrenches exerted on the object and due to the movement of the MM the object would tend to separate from the grasp. Subsequently, in order to maintain the rigid grasp (i.e. no relative movement) a wrench must be developed so that it counteracts this tendency. To incorporate the grasp condition to the mathematical models that were established in the previous sections, a mathematical description of the rigid grasp is needed. Such an expression is quite simple

$$\mathbf{x}_o = \mathbf{H}(\mathbf{q}) \quad (5.1)$$

This equation expresses that the object's pose can be defined through the manipulator's pose, while enabling for the chosen gripping point and orientation to be included.

5.1 Constraint equation

The constraint equations, described by equation 5.1 can be constructed by taking advantage of the kinematics of the manipulator as defined in the kinematics section. Referring to homogeneous transformation defined in equation 3.7, the matrix \mathbf{R}_e and vector \mathbf{p}_e describe the orientation and position of the end effector, respectively. Therefore a new homogeneous transformation matrix relating the End Effector and object frame, ${}^e\mathbf{T}_o$ must be defined, thus expressing the relative orientation and the gripping point. If the grasping of the object is done by the robot itself, through virtual servoing for example, the transformation matrix would be estimated in this form. Conversely, a predefined grasp is considered. In this case it makes sense in an intuitive framework that, as mentioned in the previous section regarding the virtual stick, the inverse transformation matrix is defined. That is

$${}^o\mathbf{T}_e = \begin{bmatrix} {}^o\mathbf{R}_e & {}^o\mathbf{p}_e \\ \mathbf{0}_{3 \times 1} & 1 \end{bmatrix} \quad (5.2)$$

Then, the needed transformation matrix will be

$${}^e\mathbf{T}_o = \begin{bmatrix} {}^o\mathbf{R}_e^T & -{}^o\mathbf{R}_e^T {}^o\mathbf{p}_e \\ \mathbf{0}_{3 \times 1} & 1 \end{bmatrix} \quad (5.3)$$

Furthermore, the rotation matrix is determined by choosing the corresponding Euler ZYX angles, ${}^o\boldsymbol{\varphi}_e = [{}^o\psi_e \quad {}^o\theta_e \quad {}^o\phi_e]$. Specifically [24]

$${}^o\mathbf{R}_e = \mathbf{R}_z(\phi)\mathbf{R}_y(\theta)\mathbf{R}_x(\psi) = \begin{bmatrix} c_\phi c_\theta & c_\phi s_\theta s_\psi - s_\phi c_\psi & c_\phi s_\theta c_\psi + s_\phi s_\psi \\ c_\phi c_\theta & c_\phi s_\theta s_\psi + s_\phi c_\psi & c_\phi s_\theta c_\psi - s_\phi s_\psi \\ -s_\theta & c_\theta s_\psi & c_\theta c_\psi \end{bmatrix} \quad (5.4)$$

where the angles notation was dropped for ease of presentation. Lastly, the homogeneous transformation describing the pose of the object through the pose of the manipulator is

$${}^W\mathbf{T}_o = {}^W\mathbf{T}_e = {}^W\mathbf{T}_V \cdot {}^V\mathbf{T}_M \cdot {}^M\mathbf{T}_e \cdot {}^e\mathbf{T}_o = \begin{bmatrix} \mathbf{R}_o & \mathbf{p}_o \\ \mathbf{0}_{1 \times 3} & 1 \end{bmatrix} \quad (5.5)$$

Then the object's generalised position vector can be synthesized by the \mathbf{p}_o vector and the orientation by choosing a minimal representation and calculating the corresponding values through the \mathbf{R}_o matrix, as done in the alternative method of the Jacobian calculation.

5.2 Case of a single manipulator

Considering equation 5.1 which imposes a constraint between the manipulator and the object, along with the dynamic equations of the manipulator, 3.64, and object, 4.13, a mathematical model of the object manipulation is defined. A proper representation of this system would be a singular system of differential equations [38] expressed as

$$\begin{bmatrix} \mathbf{M}(\mathbf{q}) & \mathbf{0} & \mathbf{0} \\ \mathbf{0} & \mathbf{M}_o & \mathbf{0} \\ \mathbf{0} & \mathbf{0} & \mathbf{0} \end{bmatrix} \begin{bmatrix} \ddot{\mathbf{q}} \\ \dot{\mathbf{v}}_o \\ \dot{\mathbf{h}}_e \end{bmatrix} = \begin{bmatrix} \mathbf{E}\boldsymbol{\tau} - \mathbf{n} + \mathbf{J}^T \mathbf{h}_e \\ -\mathbf{G}\mathbf{h}_e - \mathbf{n}_o \\ \mathbf{x}_o - \mathbf{H}(\mathbf{q}) \end{bmatrix} \quad (5.6)$$

Then, through appropriate manipulation of the system, it can be transformed to a reduced form where the interaction wrench is calculated by the combined dynamics. To perform this, consider the equation of the algebraic constraint equation 5.1, written as

$$\mathbf{Q}(\mathbf{x}) = \mathbf{x}_o - \mathbf{H}(\mathbf{q}) = \mathbf{0} \quad (5.7)$$

where $\mathbf{x} = [\mathbf{q}^T \quad \mathbf{x}_o^T]^T$. Differentiating twice, with respect to time, and applying the chain rule when it is fitting

$$\frac{d\mathbf{Q}}{d\mathbf{x}}\dot{\mathbf{x}} = 0 \Rightarrow \frac{d}{dt} \left(\frac{d\mathbf{Q}}{d\mathbf{x}} \right) \dot{\mathbf{x}} + \frac{d\mathbf{Q}}{d\mathbf{x}}\ddot{\mathbf{x}} = 0 \quad (5.8)$$

That is, the algebraic pose constraint between robot and object, propagates to an acceleration constraint. Exploiting this fact, the system of equations in 5.6 without the algebraic constraint can be solved for the combined vector of accelerations as

$$\begin{bmatrix} \mathbf{M}(\mathbf{q}) & \mathbf{0} \\ \mathbf{0} & \mathbf{M}_o \end{bmatrix} \begin{bmatrix} \ddot{\mathbf{q}} \\ \ddot{\mathbf{q}}_o \end{bmatrix} = \begin{bmatrix} \mathbf{E}\boldsymbol{\tau} - \mathbf{n} + \mathbf{J}^T \mathbf{h}_e \\ -\mathbf{G}\mathbf{h}_e - \mathbf{n}_o \end{bmatrix} \Rightarrow$$

$$\mathbf{M}(\mathbf{x})\ddot{\mathbf{x}} = \mathbf{E}(\mathbf{x})\boldsymbol{\tau} - \mathbf{n}(\mathbf{x}, \dot{\mathbf{x}}) + \mathbf{B}^T(\mathbf{x})\mathbf{h}_e \Rightarrow$$

$$\ddot{\mathbf{x}} = \mathbf{M}(\mathbf{x})^{-1} [\mathbf{E}(\mathbf{x})\boldsymbol{\tau} - \mathbf{n}(\mathbf{x}, \dot{\mathbf{x}})] + \mathbf{M}(\mathbf{x})^{-1}\mathbf{B}^T(\mathbf{x})\mathbf{h}_e \quad (5.9)$$

where the matrices of the combined system are provided by grouping and are presented for completion. Namely, the mass matrix

$$\mathbf{M}(\mathbf{x}) = \begin{bmatrix} \mathbf{M}(\mathbf{q}) & \mathbf{0} \\ \mathbf{0} & \mathbf{M}_o \end{bmatrix} \quad (5.10)$$

Coriolis-centrifugal matrix

$$\mathbf{n}(\mathbf{x}, \dot{\mathbf{x}}) = \begin{bmatrix} \mathbf{n} \\ \mathbf{n}_o \end{bmatrix} \quad (5.11)$$

the actuation related matrix

$$\mathbf{E}(\mathbf{x}) = \begin{bmatrix} \mathbf{E} \\ \mathbf{0} \end{bmatrix} \quad (5.12)$$

and the matrix applied to the wrench vector to be calculated

$$\mathbf{B}(\mathbf{x}) = [\mathbf{J} \quad -\mathbf{G}^T] \quad (5.13)$$

To avoid confusion, it is noted that when the \mathbf{x} and $\dot{\mathbf{x}}$ arguments are present, the matrices refer to the combined, manipulator and object, system. Afterwards substituting equation 5.9 in 5.8 results in

$$\frac{d}{dt} \left(\frac{d\mathbf{Q}}{d\mathbf{x}} \right) \dot{\mathbf{x}} + \frac{d\mathbf{Q}}{d\mathbf{x}} \mathbf{M}(\mathbf{x})^{-1} [\mathbf{E}(\mathbf{x})\boldsymbol{\tau} - \mathbf{n}(\mathbf{x}, \dot{\mathbf{x}})] + \frac{d\mathbf{Q}}{d\mathbf{x}} \mathbf{M}(\mathbf{x})^{-1} \mathbf{B}^T(\mathbf{x})\mathbf{h}_e = 0 \quad (5.14)$$

Then, by setting the intermediate quantities for ease of presentation

$$\boldsymbol{\Omega} = \frac{d\mathbf{Q}}{d\mathbf{x}} \mathbf{M}^{-1}(\mathbf{x}) \mathbf{B}^T(\mathbf{x}) \quad (5.15)$$

$$\boldsymbol{\Psi} = \frac{d\mathbf{Q}}{d\mathbf{x}} \mathbf{M}(\mathbf{x})^{-1} [\mathbf{n}(\mathbf{x}, \dot{\mathbf{x}}) - \mathbf{E}(\mathbf{x})\boldsymbol{\tau}] - \frac{d}{dt} \left(\frac{d\mathbf{Q}}{d\mathbf{x}} \right) \dot{\mathbf{x}} \quad (5.16)$$

the wrench can be calculated, provided that $\boldsymbol{\Omega}$ is invertible

$$\mathbf{h}_e = \boldsymbol{\Omega}^{-1} \boldsymbol{\Psi} \quad (5.17)$$

5.3 Case of multiple manipulators

The derivation of the previous section can be extended for N MMs commonly grasping an object. Consider N equations as in 3.64. Then for each manipulator the states are defined as \mathbf{q}_i , $i = 1, 2, \dots, N$. Similarly the matrices and vector used on equations of motion are denoted as $\mathbf{M}_i(\mathbf{q}_i)$, \mathbf{n}_i etc and likewise for the constraint expression $\mathbf{H}_i(\mathbf{q}_i)$. Then by stacking the aforementioned equations in block diagonal form, the system of MMs can be expressed as

$$\hat{\mathbf{M}} = \begin{bmatrix} \mathbf{M}_1(\mathbf{q}_1) & \mathbf{0} & \dots & \mathbf{0} \\ \mathbf{0} & \mathbf{M}_2(\mathbf{q}_2) & \dots & \vdots \\ \vdots & \vdots & \ddots & \mathbf{0} \\ \mathbf{0} & \dots & \mathbf{0} & \mathbf{M}_N(\mathbf{q}_N) \end{bmatrix}, \quad \hat{\mathbf{n}} = \begin{bmatrix} \mathbf{n}_1 \\ \mathbf{n}_2 \\ \vdots \\ \mathbf{n}_N \end{bmatrix} \quad (5.18)$$

$$\hat{\mathbf{E}} = \begin{bmatrix} \mathbf{E}_1 & \mathbf{0} & \dots & \mathbf{0} \\ \mathbf{0} & \mathbf{E}_2 & \dots & \vdots \\ \vdots & \vdots & \ddots & \mathbf{0} \\ \mathbf{0} & \dots & \mathbf{0} & \mathbf{E}_N \end{bmatrix}, \quad \hat{\mathbf{J}} = \begin{bmatrix} \mathbf{J}_1 & \mathbf{0} & \dots & \mathbf{0} \\ \mathbf{0} & \mathbf{J}_2 & \dots & \vdots \\ \vdots & \vdots & \ddots & \mathbf{0} \\ \mathbf{0} & \dots & \mathbf{0} & \mathbf{J}_N \end{bmatrix}$$

Then the interaction wrench, the input torque vector and the states of the multiple manipulators must be presented in a similar way as

$$\hat{\mathbf{h}}_e = \begin{bmatrix} \mathbf{h}_{e,1} \\ \mathbf{h}_{e,2} \\ \vdots \\ \mathbf{h}_{e,N} \end{bmatrix}, \quad \hat{\boldsymbol{\tau}} = \begin{bmatrix} \boldsymbol{\tau}_1 \\ \boldsymbol{\tau}_2 \\ \vdots \\ \boldsymbol{\tau}_N \end{bmatrix}, \quad \hat{\mathbf{q}} = \begin{bmatrix} \mathbf{q}_1 \\ \mathbf{q}_2 \\ \vdots \\ \mathbf{q}_N \end{bmatrix} \quad (5.19)$$

and the grasp matrix must be generalised for N grasping points as

$$\hat{\mathbf{G}} = [\mathbf{G}_1 \quad \mathbf{G}_2 \quad \dots \quad \mathbf{G}_N] \quad (5.20)$$

Lastly, the constraint equations must include the constraints relating each of the N manipulators pose to the object's pose. Therefore equation 5.7 must be also extended for N manipulator grasping an object, which is

$$\hat{\mathbf{Q}}(\mathbf{x}) = \begin{bmatrix} \mathbf{x}_o - \mathbf{H}_1(\mathbf{q}_1) \\ \mathbf{x}_o - \mathbf{H}_2(\mathbf{q}_2) \\ \vdots \\ \mathbf{x}_o - \mathbf{H}_N(\mathbf{q}_N) \end{bmatrix} = \mathbf{0} \quad (5.21)$$

Concluding, the derivation of the previous section can be generalised for N MMs carrying the object by substituting the capped matrices presented, in to equations 5.10-5.17 and taking account the extended grasp matrix and constraints.

6 Control Scheme

The dynamics of task space, as described in the respective section, have a crucial role in the handling of the object. Thus a unified approach of both the dynamics and control in task space is preferred. Furthermore, better results are achieved when a feedback linearisation scheme is used [24]. Also, as [39] concludes, the environment behaves as an admittance and, consequently, it is suitable that the control scheme imposes an impedance relation with the environment. Therefore this relation is imposed directly on the end effectors as these are the nodes of the interaction of the robot with the environment. These can be confirmed by the rich bibliography of impedance usage as [40], [32], [37], [41], [42], [15].

The impedance relation can be applied in multiple nodes and it is deemed a design choice. It is worth mentioning that in [43] a comparison between Multiple Impedance Control (MIC) and Object Impedance Control (OIC) is made. The former applies the impedance relation in both the object coordinates and to all the end effectors, while the latter only applies the impedance on the object. It is concluded that the MIC algorithm shows better performance, considering same gains, as well as better path tracking. Therefore, a MIC scheme is utilized based in [37], [44] and [36].

Considering N Mobile Manipulators gripping the object and equation 3.66 the input wrench of the i -th manipulator can be decomposed as

$$\mathbf{u}_i = \mathbf{u}_{m,i} + \mathbf{u}_{f,i} \quad (6.1)$$

where $\mathbf{u}_{m,i}$ is the applied control force causing motion of the End Effector and $\mathbf{u}_{f,i}$ is the required force to be applied on the object by the i -th end effector. The desired impedance relationship for the object motion is

$$\mathbf{M}_{des}\ddot{\mathbf{e}} + \mathbf{K}_d\dot{\mathbf{e}} + \mathbf{K}_p\mathbf{e} = \mathbf{h}_{o,env} \quad (6.2)$$

where $\mathbf{e} = \mathbf{x}_{des} - \mathbf{x}_o$ is the error of the object states and similarly for the derivatives. \mathbf{M}_{des} , \mathbf{K}_d , \mathbf{K}_p are diagonal gain matrices of appropriate size. Also, in the right hand side, the wrench, $\mathbf{h}_{o,env}$, of the desired impedance is the forces and moments acting on the object due to the interaction with the environment. In that way, the error will have a dynamic relation with the actual forces experienced from the system, specifically from the transportation of the object. Considering the object dynamics 4.8 the desired impedance can be obtained if the total wrench of the N Mobile Manipulators on the object is

$$\hat{\mathbf{G}}\hat{\mathbf{h}}_e = \mathbf{M}_o\mathbf{M}_{des}^{-1} [\mathbf{M}_{des}\ddot{\mathbf{x}}_{o,des} + \mathbf{K}_d\dot{\mathbf{e}} + \mathbf{K}_p\mathbf{e} - \mathbf{h}_{o,env}] + \mathbf{n}_o \quad (6.3)$$

Thus achieving the feedback linearisation by cancelling the velocity and position terms, leaving only the inertial terms. Next, through the pseudo-inverse of the Grasp matrix, the input wrench needed from each manipulator is calculated as

$$\mathbf{u}_f = \hat{\mathbf{G}}^\# \hat{\mathbf{G}}\hat{\mathbf{h}}_e + (\mathbf{I} - \hat{\mathbf{G}}^\# \hat{\mathbf{G}})\mathbf{h}_I \quad (6.4)$$

where $\mathbf{u}_f = [\mathbf{u}_{f,1}^T \ \mathbf{u}_{f,2}^T \ \dots \ \mathbf{u}_{f,N}^T]^T$ and \mathbf{h}_I is defined similarly, containing the internal forces experienced by the object. This particular computation requires

knowledge of the contact forces and for the needs of this study the model used in the dynamic equations was considered. For applications in a physical system and on-line computation of the contact forces finite differences approximation can be used [37]. The inputs calculated for each EE from equation 6.4 are the force inputs. Next, imposing the same impedance relationship in each EE and performing a similar derivation the motion inputs of each manipulator are

$$\mathbf{u}_{m,i} = \tilde{\mathbf{M}}\mathbf{M}_{des}^{-1} \left[\mathbf{M}_{des}\ddot{\mathbf{x}}_{des,i} + \mathbf{K}_d\dot{\tilde{\mathbf{e}}}_i + \mathbf{K}_p\tilde{\mathbf{e}}_i - \mathbf{h}_{I,i} \right] + \tilde{\mathbf{n}} \quad (6.5)$$

where $\mathbf{e} = \mathbf{x}_{des} - \mathbf{x}_o$ is the error of the EE states and similarly for the derivatives, $\mathbf{h}_{I,i}$ is the contribution of the i-th EE to the internal force of the object [36], i.e. the i-th component of the total internal wrench vector. Lastly, it is noted that simulation analyses have shown that the best results are obtained by choosing the same impedance parameters for both the object and the end effectors. This is easily explained by the harmonious motion that is ensured by the same error dynamics [37].

7 Simulation and Results

7.1 Software

MATLAB[®] and Simulink[®] were used for this analysis, along with the Symbolic Toolbox, in order to produce the matrices of the dynamic equations produced in the corresponding sections. The work aimed to provide a generalised algorithm that will be able to be utilised in multiple scenarios by allowing easy computation of the kinematics and dynamics of the system and by extension fast simulation to be possible. More info about the structure of the algorithm and the functions that were created can be found on the appendix.

7.2 Results

To verify the software that was developed, a simulation scenario is tested. Specifically, two identical MMs rigidly grasp an object. The Mobile Manipulators consist of a vehicle and a 1-DoF manipulator. The DoF is a revolute joint producing a rotation with respect to the plane on which the platform is moving. By extension,

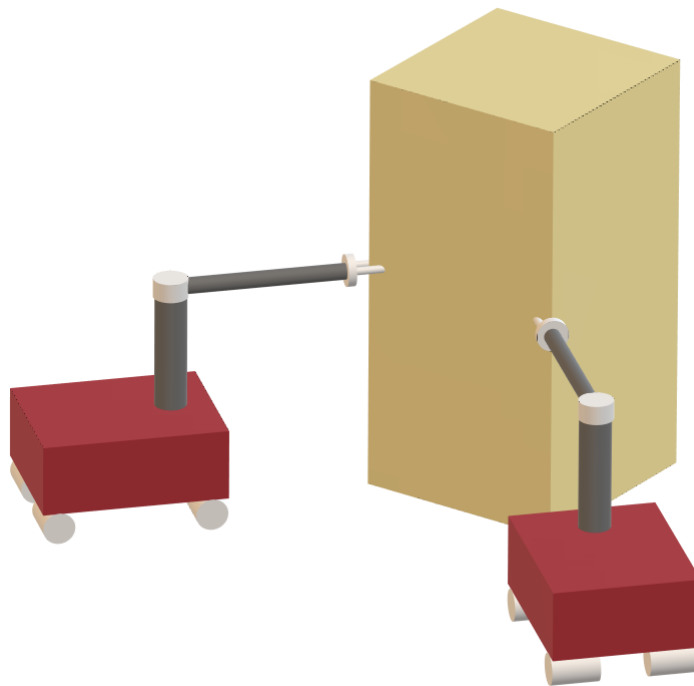


Figure 7.1: Case of two Mobile Manipulators cooperatively handling an object

only the planar DoFs of the object are considered. Therefore, due to the 3+1 DoFs of the MM and the 3 DoFs of the object, or equivalently task space, the MM is redundant. Also, internal grasping wrenches are considered zero. First, an object trajectory consisting of X and Y coordinates along with the orientation of it are produced. At first sinusoidal and circular trajectories with constant orientation

are considered. For the circular case it was also considered to have a variable orientation such that it is always tangent to the circular trajectory. Then, through the object kinematics described by 4.1 and 4.2, the corresponding End Effector trajectories are computed. These are then fed to the control algorithm, which by considering the f/t measurement, send the proper input to the actuators. Moreover, regarding f/t measurements, a 5% deviation around the calculated value and a delay of 10ms was considered. The object is assumed rectangular and with a mass of $m_0 = 100kg$ and an inertia of $I_0 = 4.3kgm^2$. Object shape is of concern only for path planning where collision avoidance is studied. This can be accomplished by integrating artificial potential navigation functions in the path planning algorithm, introduced by [45]. Similar examples of these methodologies include [46], [47], [48] and path planning algorithms for cooperative manipulation for MMs have been proposed [49], [50], [51]. Nevertheless, in this study a predetermined trajectory is given to the control algorithm. For the friction coefficients logical values were used. Further, the gains of the impedances were selected appropriately as

$$\begin{aligned}\mathbf{M}_{des} &= 100\mathbf{I}_{3\times 3} \\ \mathbf{K}_d &= 800\mathbf{I}_{3\times 3} \\ \mathbf{K}_p &= 600\mathbf{I}_{3\times 3}\end{aligned}$$

considering the convergence of the trajectory, the total time and error and dynamical behaviour of the system. The controller sufficiently tracks the desired path and converges, although with a steady state error, which is to be expected due to the lack of integral action on the control law that would eliminate the steady state error. Below, multiple graphs for each trajectory are presented. Specifically, the object path and error along with the end effectors errors and inputs are included. Also, for the circular path the animation of the object transportation in planar view can be found at <https://vimeo.com/679978059> and in 3D view at <https://vimeo.com/679977704>.

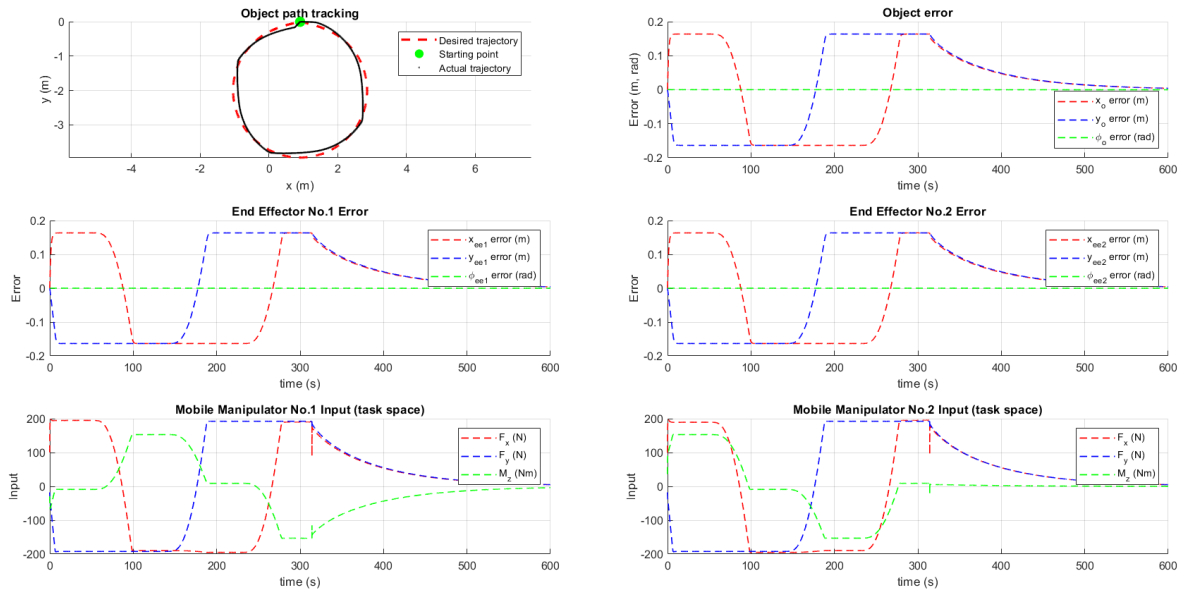


Figure 7.2: Circular Trajectory Simulation with constant orientation

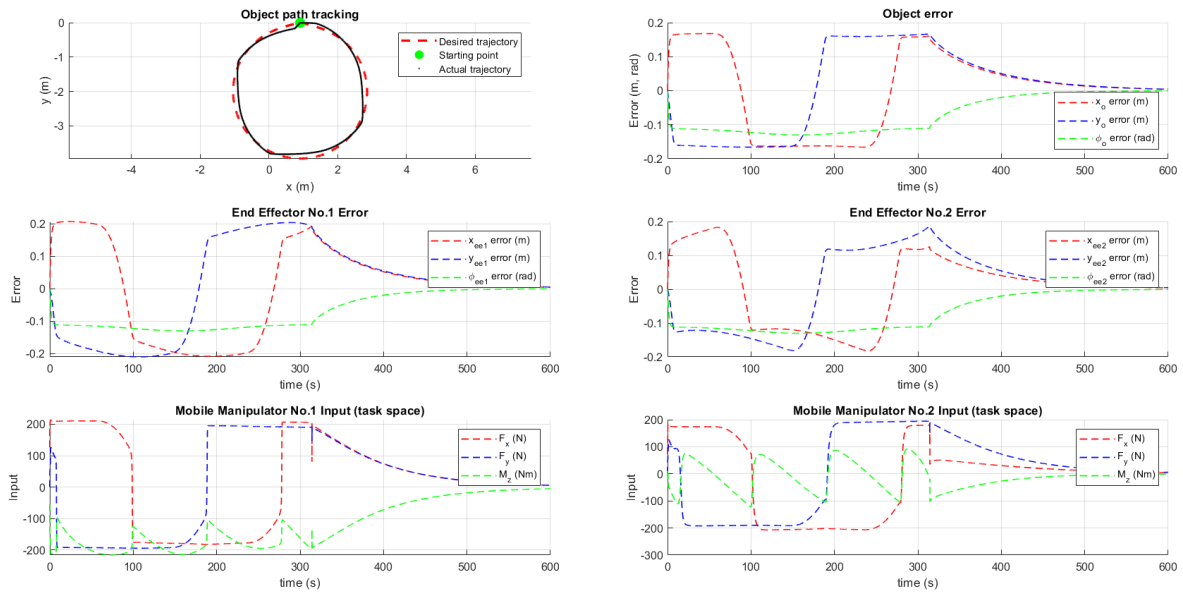


Figure 7.3: Circular Trajectory Simulation with variable orientation

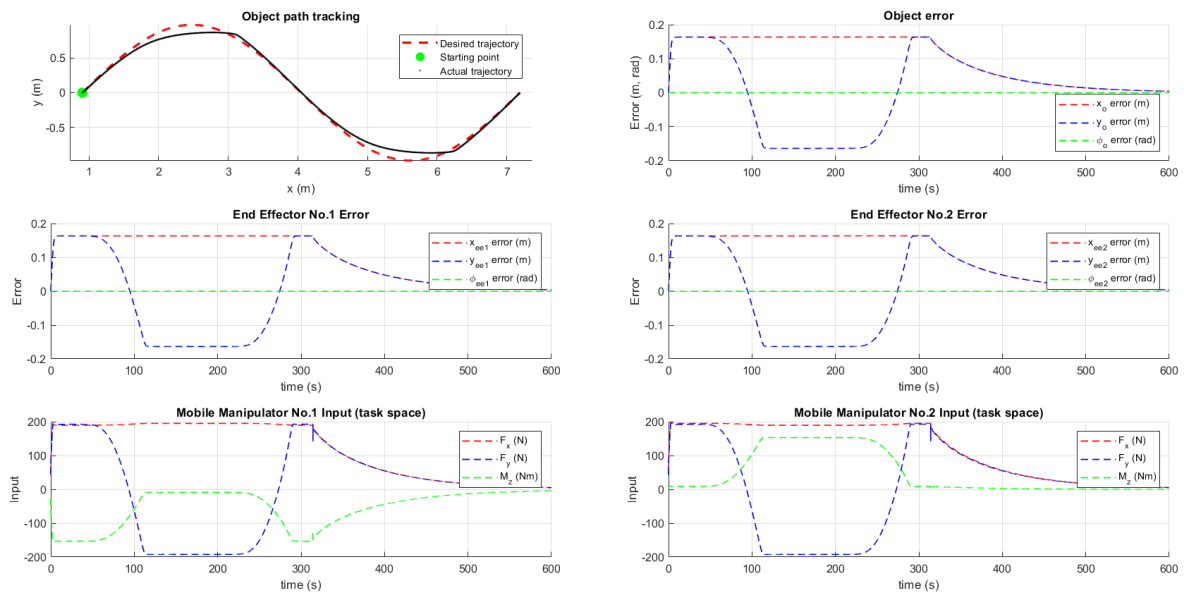


Figure 7.4: Sinusoidal Trajectory Simulation with constant orientation

8 Conclusion

In this study a parametric model was constructed aiming at the development of a tool to ease the modelling procedure of these complex systems. The prerequisites of the tool include the kinematic and dynamic model of the vehicle along with the parameters of a typical manipulator, i.e. inertial characteristics and the Denavit-Hartenberg table. The matrices describing the dynamic behaviour of a mobile robot and the object, along with the constraint related functions are then outputted.

The grip was considered rigid which gave rise to a mathematical description of the robot-object interaction, that is an algebraic relationship of the respective variables. Then the differential-algebraic system was able to be reduced in order to efficiently simulate the task. Here, it is noted that additional algebraic constraints can be set, e.g. in order to accommodate the movement of the object on an arbitrary manifold. Consequently, by following the same procedure, the system can be reduced leading to both the robot-object and object-manifold interactions to be calculated. The control scheme, was based on the impedance framework as the goal is to control the object movement, which is achieved by controlling the forces that are applied from the robots to the object.

In the last section, a cooperative transportation of an object, under planar movement constraint, was achieved through a centralized scheme where only robotic agents were used. The trajectories that were selected for the simulations were satisfactorily tracked. This further validates the dynamic model that was developed and renders it a tool in relevant research. Such research consists mainly of software development. Namely algorithms that either work towards making mobile robots autonomous, such as with decentralized cooperation schemes, or providing them with the appropriate intelligence in order to cooperate with human agents such as appropriate interpretation of f/t measurements regarding the human agents' intentions.

Εκτενής Περίληψη Διπλωματικής Εργασίας

Μοντελοποίηση Κινητού Χειριστή

Γενικά, η μαθηματική μοντελοποίηση ενός Χειριστή, βασίζεται στην κινηματική, διαφορική κινηματική και δυναμική ανάλυση. Κατ' αναλογία, στη περίπτωση του Κινητού Χειριστή θα πρέπει να πραγματοποιηθούν οι παραπάνω αναλύσεις. Αναφέρεται ότι ένας Κινητός Χειριστής αποτελείται από το όχημα ή αλλιώς την Κινητή Πλατφόρμα και τον Χειριστή, ο οποίος είναι στερεωμένος πάνω σε αυτή. Η διακριτοποίηση αυτή, άμεσα παραπέμπει στην ύπαρξη δύο υπο-συστημάτων. Επιπλέον, στη βιβλιογραφία υπάρχει πλήθος μοντέλων οχημάτων ενώ η μοντελοποίηση των Χειριστών είναι σχεδόν τυποποιημένη ένεκα της σύμβασης Denavit-Hartenberg. Επομένως, είναι προς όφελος της παραμετροποίησης τα μοντέλα που αναφέρθηκαν για τον Κινητό Χειριστή να προκύπτουν με χρήση των αντίστοιχων μοντέλων της Πλατφόρμας και του Χειριστή. Με αυτό το σκεπτικό ορίζονται τα εξής Συστήματα Συντεταγμένων:

- το αδρανειακό Σύστημα Συντεταγμένων $\{W\}$
- το Σύστημα Συντεταγμένων της Κινητής Πλατφόρμας $\{V\}$, τοποθετημένο στο κεντροειδές και
- η αλληλουχία Συστημάτων Συντεταγμένων από το $\{0\}$ ή $\{M\}$ στο $\{n\}$ ή $\{E\}$ Σύστημα Συντεταγμένων, τοποθετημένα στις αρθρώσεις του Χειριστή, σύμφωνα με τη σύμβαση DH.

Κινηματική

Η κινηματική ανάλυση της Πλατφόρμας βασίζεται στην μελέτη του Συστήματος Συντεταγμένων $\{V\}$ ως προς το ακίνητο $\{W\}$ που εκφράζεται μέσω του αντίστοιχου πίνακα Ομογενή Μετασχηματισμού. Οι μεταβλητές που περιγράφουν τη κίνηση της Πλατφόρμας είναι $\mathbf{q}_v = [q_{v,1} \ q_{v,2} \ \dots \ q_{v,n}]^T$, \mathbf{n}_v το πλήθος. Στη περίπτωση που θα μελετηθεί η Πλατφόρμα δύναται να κινηθεί αποκλειστικά επι του επιπέδου, οπότε $n_v = 3$ και $\mathbf{q}_v = [x_v \ y_v \ \phi]^T$ και τότε ο Ομογενής Μετασχηματισμός ορίζεται ως

$${}^W\mathbf{T}_V = {}^W\mathbf{T}_V(\mathbf{q}_v) = \begin{bmatrix} \mathbf{R}_V & \mathbf{r}_V \\ \mathbf{0}_{1 \times 3} & 1 \end{bmatrix}$$

Όπου ο προσανατολισμός, λόγω της κίνησης σε επίπεδο, είναι

$$\mathbf{R}_V = \mathbf{R}_V(\phi) = \begin{bmatrix} \cos \phi & -\sin \phi & 0 \\ \sin \phi & \cos \phi & 0 \\ 0 & 0 & 1 \end{bmatrix}$$

και η μεταφορά εκφράζεται από το διάνυσμα $\mathbf{r}_v = [x_v \ y_v \ z_v]^T$ και συγκεκριμένα από τις δύο πρώτες συνιστώσες. Η τρίτη συνιστώσα, z_v , στην περίπτωση αυτή, είναι μία σταθερή μετατόπιση λόγω της απόστασης του κεντροειδούς από το έδαφος. Έπειτα, ο Μετασχηματισμός μεταξύ της Κινητής Πλατφόρμας και της βάσης του Χειριστή

πρέπει να οριστεί. Θεωρείται ότι τα Συστήματα Συντεταγμένων, είναι τοποθετημένα με τον ίδιο προσανατολισμό ως

$${}^V\mathbf{T}_W = \begin{bmatrix} \mathbf{I}_{3 \times 3} & \mathbf{r}_{rp} \\ \mathbf{0}_{1 \times 3} & 1 \end{bmatrix}$$

όπου το διάνυσμα \mathbf{r}_{rp} εκφράζει την σταθερή απόσταση των δύο Συστημάτων Συντεταγμένων. Ακολούθως, ως προς τον Χειριστή, η σύμβαση Denavit-Hartenberg περιγράφει την θέση και τον προσανατολισμό του ακροδέκτη ως προς ένα σύστημα που συνήθως τοποθετείται στη βάση του Χειριστή. Ένα Σύστημα Συντεταγμένων τοποθετείται σε κάθε άρθρωση και επιλέγονται οι τέσσερις παράμετροι που ορίζονται από τη σύμβαση. Οι μεταβλητές των αρθρώσεων, οι οποίες είναι είτε γωνιακές είτε γραμμικές μετατοπίσεις, ορίζονται ως $\mathbf{q}_r = [q_{r1} \ q_{r2} \ \dots \ q_{rn}]^T$, ενώ οι παράμετροι της σύμβασης δίνονται σε μορφή πίνακα

Link i	a_i	α_i	d_i	θ_i
1				
2				
⋮				
n_r				

Πίνακας 1: Πίνακας Παραμέτρων Denavit-Hartenberg

και οι επιμέρους Μετασχηματισμοί ορίζονται ως

$${}^{i-1}\mathbf{T}_i = \begin{bmatrix} \cos \theta_i & -\cos \alpha_i \sin \theta_i & \sin \alpha_i \sin \theta_i & a_i \cos \theta_i \\ \sin \theta_i & \cos \alpha_i \cos \theta_i & -\sin \alpha_i \cos \theta_i & a_i \sin \theta_i \\ 0 & \sin \alpha_i & \cos \alpha_i & d_i \\ 0 & 0 & 0 & 1 \end{bmatrix}$$

ενώ ο συνολικός Μετασχηματισμός από τη βάση στον ακροδέκτη του Χειριστή μπορεί να παρασταθεί συνοπτικότερα ως

$${}^M\mathbf{T}_e = {}^M\mathbf{T}_e(\mathbf{q}_r) = {}^0\mathbf{T}_n = {}^0\mathbf{T}_1 \cdot {}^1\mathbf{T}_2 \cdot \dots \cdot {}^{n-1}\mathbf{T}_n$$

Τέλος για να ολοκληρωθεί η κινηματική ανάλυση πρέπει να εκφραστεί η πόζα του ακροδέκτη σε σχέση με το αδρανειακό Σύστημα Συντεταγμένων. Επομένως, σύμφωνα με τα προηγούμενα μπορεί να οριστεί ένας ολικός Ομογενής Μετασχηματισμός

$${}^W\mathbf{T}_e = {}^W\mathbf{T}_V \cdot {}^V\mathbf{T}_M \cdot {}^M\mathbf{T}_e$$

Διαφορική Κινηματική

Η Διαφορική Κινηματική ενός ρομποτικού βραχίονα εκφράζεται μέσω της Ιακωβιανής και συσχετίζει την ταχύτητα, ως προς τη βάση, του ακροδέκτη με τις ταχύτητες των αρθρώσεων και ορίζεται ως

$${}^V\dot{\mathbf{x}}_e^M = \begin{bmatrix} V \dot{\mathbf{p}}_e^M \\ V \boldsymbol{\omega}_e^M \end{bmatrix} = \mathbf{J}_{FB} \dot{\mathbf{q}}_r$$

Ονομάζεται Γεωμετρική Ιακωβιανή μπορεί να γραφτεί κατά μέρη που σχετίζονται με τους γραμμικούς και περιστροφικούς βαθμούς ελευθερίας

$$\mathbf{J}_{FB} = \begin{bmatrix} \mathbf{J}_P \\ \mathbf{J}_O \end{bmatrix}$$

Παραγωγίζοντας τις σχέσεις της ευθείας κινηματικής που παρουσιάστηκαν προηγουμένως, δύνатаι να υπολογιστεί [24] η κάθε στήλη της Ιακωβιανής ως

$$\begin{bmatrix} \mathbf{J}_{Pi} \\ \mathbf{J}_{Oi} \end{bmatrix} = \begin{cases} \begin{bmatrix} \mathbf{z}_{i-1} \\ \mathbf{0} \end{bmatrix} & \text{για πρισματική άρθρωση} \\ \begin{bmatrix} \mathbf{z}_{i-1} \times (\mathbf{p}_e - \mathbf{p}_{i-1}) \\ \mathbf{z}_{i-1} \end{bmatrix} & \text{για περιστροφική άρθρωση} \end{cases}$$

Δεδομένου ότι σε πολλές περιπτώσεις η Ιακωβιανή ενός Χειριστή είναι εκ των προτέρων γνωστή, κρίνεται σκόπιμο να χρησιμοποιηθεί στη Διαφορική Κινηματική ανάλυση του Κινητού Χειριστή. Αυτό μπορεί να γίνει με κατάλληλη χειραγώγηση των εξισώσεων κινηματικής

$$\begin{aligned} \boldsymbol{\omega}_e &= \boldsymbol{\omega}_V + \boldsymbol{\omega}_e^V \\ \dot{\mathbf{p}}_e &= \dot{\mathbf{p}}_V + \boldsymbol{\omega}_V \times \mathbf{p}_e^V + \dot{\mathbf{p}}_e^V \\ \dot{\mathbf{p}}_e^V &= \dot{\mathbf{p}}_e^M + \dot{\mathbf{p}}_M^V \end{aligned}$$

Επειδή ο Χειριστής είναι στερεά τοποθετημένος στην Πλατφόρμα $\mathbf{r}_M^V = 0$. Έπειτα, λαμβάνοντας υπόψη τη κινηματική ανάλυση της Πλατφόρμας μπορούν να γραφούν οι σχέσεις

$$\begin{aligned} \mathbf{p}_e^V &= \mathbf{R}_V^V \mathbf{p}_e^V \\ \dot{\mathbf{p}}_e^M &= \mathbf{R}_V^V \dot{\mathbf{p}}_e^M \\ \boldsymbol{\omega}_e^V &= \boldsymbol{\omega}_e^M = \mathbf{R}_V^V \boldsymbol{\omega}_e^M \end{aligned}$$

Τελικά με συνδυασμό των προηγούμενων εξισώσεων

$$\dot{\mathbf{x}}_e = \begin{bmatrix} \dot{\mathbf{p}}_e \\ \boldsymbol{\omega}_e \end{bmatrix} = \begin{bmatrix} \dot{\mathbf{p}}_V \\ \boldsymbol{\omega}_V \end{bmatrix} + \begin{bmatrix} [\boldsymbol{\omega}_V]_{\times} \mathbf{R}_V^V \mathbf{p}_e^V \\ \boldsymbol{\omega}_e \end{bmatrix} + \begin{bmatrix} \mathbf{R}_V^V \dot{\mathbf{p}}_e^M \\ \mathbf{R}_V^V \boldsymbol{\omega}_e^M \end{bmatrix}$$

όπου το $[\cdot]_{\times}$ συμβολίζει τον αντι-συμμετρικό πίνακα ο οποίος εκφράζει το εξωτερικό γινόμενο. Χρησιμοποιώντας κάποιες από τις ιδιότητες του εξωτερικού γινόμενου η παραπάνω έκφραση μπορεί να πάρει τη μορφή

$$\dot{\mathbf{x}}_e = \begin{bmatrix} \dot{\mathbf{p}}_e \\ \boldsymbol{\omega}_e \end{bmatrix} = \begin{bmatrix} \mathbf{I} & -\mathbf{R}_V^V [\mathbf{p}_e^V]_{\times} \mathbf{R}_V^T \\ \mathbf{0} & \mathbf{I} \end{bmatrix} \begin{bmatrix} \dot{\mathbf{p}}_V \\ \boldsymbol{\omega}_V \end{bmatrix} + \begin{bmatrix} \mathbf{R}_V^V & \mathbf{0} \\ \mathbf{0} & \mathbf{R}_V^V \end{bmatrix} \begin{bmatrix} \dot{\mathbf{p}}_e^M \\ \boldsymbol{\omega}_e^M \end{bmatrix}$$

Η σχέση Διαφορικής Κινηματικής, που εκφράζει τη θέση και τη γωνιακή ταχύτητα του ακροδέκτη, μπορεί να γραφεί με τη συνήθη μορφή ως

$$\dot{\mathbf{x}}_e = \begin{bmatrix} \dot{\mathbf{p}}_e \\ \boldsymbol{\omega}_e \end{bmatrix} = \begin{bmatrix} \mathbf{J}_v & \mathbf{J}_r \end{bmatrix} \begin{bmatrix} \dot{\mathbf{q}}_v \\ \dot{\mathbf{q}}_r \end{bmatrix} = \mathbf{J} \dot{\mathbf{q}}$$

όπου από τα προηγούμενα, άμεσα προκύπτει ότι

$$\mathbf{J}_v = \begin{bmatrix} \mathbf{I} & -\mathbf{R}_V \begin{bmatrix} V \mathbf{p}_e^V \\ \times \end{bmatrix} \mathbf{R}_V^T \\ \mathbf{0} & \mathbf{I} \end{bmatrix}$$

$$\mathbf{J}_r = \begin{bmatrix} \mathbf{R}_V & \mathbf{0} \\ \mathbf{0} & \mathbf{R}_V \end{bmatrix} \mathbf{J}_{FB}$$

Σημειώνεται ότι η Γεωμετρική Ιακωβιανή δύναται να βρεθεί και με έναν ακόμα τρόπο. Συγκεκριμένα μπορεί να υπολογιστεί μέσω της Αναλυτικής Ιακωβιανής, \mathbf{J}_A . Πρώτα εκφράζεται η θέση, \mathbf{p}_e , και ο προσανατολισμός του ακροδέκτη, φ_e , μέσω της ευθείας κινηματικής. Σημειώνεται ότι για τον προσανατολισμό πρέπει να επιλεγεί μία ελαχιστοτική παράσταση με τη πιο συνηθισμένη να είναι η ZYX (Roll-Pitch-Yaw). Έπειτα οι σχέσεις παραγωγίζονται και λαμβάνεται η έκφραση των ταχυτήτων. Όμως η τυπική Ιακωβιανή αναφέρεται στην γωνιακή ταχύτητα και όχι στην παράγωγο του προσανατολισμού. Ως εκ τούτου, είναι αναγκαία μία σχέση που να συνδέει αυτές τις ταχύτητες και έχει τη μορφή

$$\boldsymbol{\omega}_e = \mathbf{T}(\varphi_e) \dot{\varphi}_e$$

Τότε παρατηρώντας τις σχέσεις ορισμού της Γεωμετρικής και Αναλυτικής Ιακωβιανής, αυτές συνδέονται μέσω της σχέσης

$$\mathbf{J} = \begin{bmatrix} \mathbf{I}_{3 \times 3} & \mathbf{0}_{3 \times 3} \\ \mathbf{0}_{3 \times 3} & \mathbf{T}(\varphi_e) \end{bmatrix} \mathbf{J}_A = \mathbf{T}_A \mathbf{J}_A$$

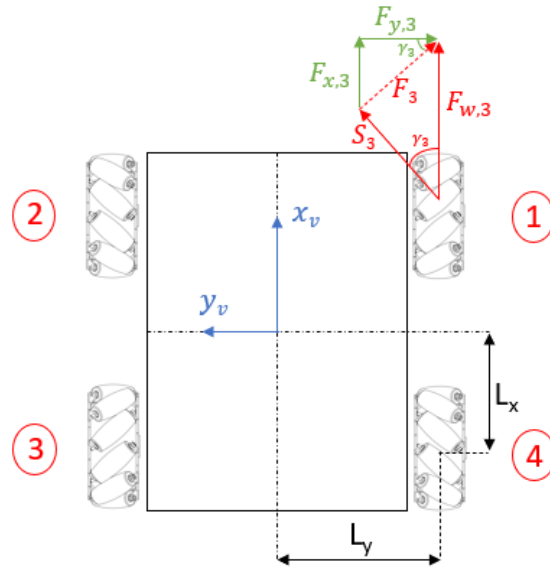
όπου ο πίνακας $\mathbf{T}(\varphi_e)$ μπορεί να προκύψει με κατάλληλη ανάλυση της ελαχιστοτικής αναπαράστασης που επιλέχθηκε.

Δυναμική

Επιλέγεται μία απλοποιητική μοντελοποίηση λόγω των χαμηλών ταχυτήτων με τις οποίες θα κινείται. Η Κινητή Πλατφόρμα μπορεί να θεωρηθεί ως μάζα σε επίπεδη κίνηση όπου λαμβάνεται υπόψη μόνο η αδράνεια, καθώς και η επενέργεια, η οποία προκύπτει από τη περιστροφή των ροδών. Η Κινητή Πλατφόρμα διαθέτει τέσσερις ολονομικές ρόδες τύπου Mecanum. Σε κάθε ροδά, κατά τη περιστροφή, αναπτύσσεται δύναμη που παράγει έργο με προσανατολισμό ίδιο με εκείνο των κυλίνδρων που διαθέτουν οι ρόδες. Έπειτα αυτή η δύναμη αναλύεται στις κατευθύνσεις των αξόνων του Συστήματος Συντεταγμένων που είναι τοποθετημένο στην Πλατφόρμα. Γνωρίζοντας τις δυνάμεις μπορεί να υπολογιστεί και η ροπή που προκαλεί κάθε μία εξ' αυτών. Τέλος οι συνολικές δυνάμεις στις δύο διευθύνσεις και η συνολική ροπή προκύπτουν με άθροιση της συνεισφοράς κάθε ρόδας. Το δυναμικό μοντέλο της Πλατφόρμας είναι

$$\mathbf{M}_{v1} \ddot{\mathbf{q}}_v = \mathbf{E}_v \boldsymbol{\tau}_w - \mathbf{D}_v$$

όπου ο πίνακας \mathbf{M}_{v1} είναι το (διαγώνιο) μητρώο μάζας και είναι σταθερό. Ο πίνακας \mathbf{E}_v αναφέρεται σε κατάλληλο πίνακα που μετασχηματίζει τις ροπές στις ρόδες σε κατάλληλα μεγέθη επενέργειας στους βαθμούς ελευθερίας της Κινητής Πλατφόρμας. Τέλος ο πίνακας \mathbf{D}_v παριστάνει τη στατική τριβή που δέχεται η πλατφόρμα λόγω της επαφής των ροδών με το έδαφος. Ο Χειριστής που τοποθετείται στη Πλατφόρμα



Σχήμα 1: Κινητή Πλατφόρμα με 4 ρόδες τύπου Mecanum

διαθέτει, συνήθως, πολλούς Βαθμούς Ελευθερίας οπότε πρέπει να χρησιμοποιηθεί μία συστημική μέθοδος για τον υπολογισμό των δυναμικών εξισώσεων. Η μέθοδος Euler-Lagrange είναι η πλέον ενδεδειγμένη. Αρχικά \mathcal{K} και \mathcal{V} είναι η συνολική κινητική και δυναμική ενέργεια αντίστοιχα. Τότε η Λαγκραντζιανή ορίζεται ως

$$\mathcal{L}(\mathbf{q}_r, \dot{\mathbf{q}}_r) = \mathcal{K}(\mathbf{q}_r, \dot{\mathbf{q}}_r) - \mathcal{V}(\mathbf{q}_r)$$

Οι εξισώσεις κίνησης του Χειριστή προκύπτουν από τις σχέσεις

$$\frac{d}{dt} \frac{\partial \mathcal{L}}{\partial \dot{q}_{r,i}} - \frac{\partial \mathcal{L}}{\partial q_{r,i}} = \tau_{r,i} \quad i = 1, 2, \dots, n_r$$

όπου $\tau_{r,i}$ είναι η γενικευμένη δύναμη που αντιστοιχεί στη γενικευμένη θέση $q_{r,i}$. Η κινητική και δυναμική ενέργεια του i -στου συνδέσμου του Χειριστή είναι

$$\mathcal{K}_i = \frac{1}{2} \text{trace} \left[\sum_{j=1}^i \sum_{k=1}^i \frac{\partial \mathbf{T}_i}{\partial q_{r,j}} \mathbf{J}_i \frac{\partial \mathbf{T}_i^T}{\partial q_{r,k}} \dot{q}_{r,j} \dot{q}_{r,k} \right]$$

$$\mathcal{V}_i = -m_i \mathbf{g}^T \mathbf{T}_i \bar{\mathbf{r}}_i$$

όπου $\mathbf{T}_i = {}^0\mathbf{T}_1 \cdot {}^1\mathbf{T}_2 \cdot \dots \cdot {}^{i-1}\mathbf{T}_i$. Ακόμα, \mathbf{J}_i και m_i είναι το μητρώο Ψευδο-Αδράνειας [31] και η μάζα του συνδέσμου i , αντίστοιχα, \mathbf{g}^T είναι το διάνυσμα της βαρυτικής επιτάχυνσης ως προς τη βάση του Χειριστή και $\bar{\mathbf{r}}_i$ είναι το διάνυσμα με κατεύθυνση από το Σύστημα Συντεταγμένων i στο κεντροειδές του συνδέσμου i εκπεφρασμένο στο Σύστημα Συντεταγμένων i .

Από τις παραπάνω εξισώσεις και με τους κατάλληλους υπολογισμούς προκύπτουν οι εξισώσεις κίνησης του Χειριστή ως

$$\sum_{j=1}^{n_r} M_{ij} \ddot{q}_{r,j} + \sum_{j=1}^{n_r} \sum_{k=1}^{n_r} C_{ijk} \dot{q}_{r,j} \dot{q}_{r,k} + G_i = \tau_{r,i}$$

όπου

$$M_{ij} = \sum_{k=\max(i,j)}^{n_r} \text{trace} \left[\frac{\partial \mathbf{T}_k}{\partial q_{r,i}} \mathbf{J}_k \frac{\partial \mathbf{T}_k^T}{\partial q_{r,j}} \right]$$

$$C_{ijk} = \sum_{h=\max(i,j,k)}^{n_r} \text{trace} \left[\frac{\partial \mathbf{T}_h}{\partial q_{r,i}} \mathbf{J}_h \frac{\partial^2 \mathbf{T}_h^T}{\partial q_{r,j} \partial q_{r,k}} \right]$$

$$G_i = \sum_{k=i}^{n_r} m_k \mathbf{g}^T \frac{\partial \mathbf{T}_k}{\partial q_{r,i}} \bar{\mathbf{r}}_i$$

Επιπλέον, προστίθεται και όρος ιξώδους τριβής που συνήθως μοντελοποιείται στους Χειριστές

$$\mathbf{M}_{r1}(\mathbf{q}_r) \ddot{\mathbf{q}}_r + \mathbf{C}_{r1}(\mathbf{q}_r, \dot{\mathbf{q}}_r) + \mathbf{G}_r(\mathbf{q}_r) + \mathbf{D}_r \dot{\mathbf{q}}_r = \boldsymbol{\tau}_r$$

όπου $\mathbf{q}_r = [q_{r,1} \ q_{r,2} \ \dots \ q_{r,n}]^T$ και \mathbf{D}_r διαγώνιος πίνακας με τους συντελεστές ιξώδους τριβής. Οι προηγούμενες εξισώσεις περιγράφουν την αυτοσία δυναμική των υποσυστημάτων του συνολικού συστήματος, ήτοι της Κινητής Πλατφόρμας και του Χειριστή. Οι δυναμικές εξισώσεις του συστήματος προκύπτουν από εκείνες των υποσυστημάτων μαζί με τους κατάλληλους όρους που εκφράζουν την αλληλεπίδραση και επίδραση του ενός στο άλλο. Αυτή τη φορά ισχύει $\mathbf{T}_i = {}^W \mathbf{T}_V \cdot {}^V \mathbf{T}_M \cdot {}^0 \mathbf{T}_1 \cdot {}^1 \mathbf{T}_2 \cdot \dots \cdot {}^{i-1} \mathbf{T}_i$. Αρχικά οι επιπρόσθετοι όροι Coriolis που εμφανίζονται στον Χειριστή λόγω της Πλατφόρμας είναι

$$C_{r2}(i) = 2 \sum_{j=1}^{n_v} \sum_{k=1}^{n_r} \sum_{h=\max(i,k)}^{n_r} \text{trace} \left[\frac{\partial \mathbf{T}_h}{\partial q_{r,i}} \mathbf{J}_h \frac{\partial^2 \mathbf{T}_h^T}{\partial q_{v,j} \partial q_{r,k}} \right] \dot{q}_{v,j} \dot{q}_{r,k}$$

$$+ \sum_{j=1}^{n_v} \sum_{k=1}^{n_v} \sum_{h=i}^{n_r} \text{trace} \left[\frac{\partial \mathbf{T}_h}{\partial q_{r,i}} \mathbf{J}_h \frac{\partial^2 \mathbf{T}_h^T}{\partial q_{v,j} \partial q_{v,k}} \right] \dot{q}_{v,j} \dot{q}_{v,k}$$

και η επίδραση στη κίνηση

$$R_r(i, j) = \sum_{k=i}^{n_v} \text{trace} \left[\frac{\partial \mathbf{T}_k}{\partial q_{r,i}} \mathbf{J}_k \frac{\partial \mathbf{T}_k^T}{\partial q_{v,j}} \right] \quad 1 \leq i \leq n_r, 1 \leq j \leq n_v$$

Αντίστοιχα, οι επιπλέον όροι για τη Κινητή Πλατφόρμα θα είναι

$$M_{v2}(i, j) = \sum_{k=1}^{n_r} \text{trace} \left[\frac{\partial \mathbf{T}_k}{\partial q_{v,i}} \mathbf{J}_k \frac{\partial \mathbf{T}_k^T}{\partial q_{v,j}} \right] \quad 1 \leq i, j \leq n_v$$

$$C_{v2}(i) = 2 \sum_{j=1}^{n_r} \sum_{k=1}^{n_v} \sum_{h=j}^{n_r} \text{trace} \left[\frac{\partial \mathbf{T}_h}{\partial q_{v,i}} \mathbf{J}_h \frac{\partial^2 \mathbf{T}_h^T}{\partial q_{r,j} \partial q_{v,k}} \right] \dot{q}_{r,j} \dot{q}_{v,k}$$

$$+ \sum_{j=1}^{n_r} \sum_{k=1}^{n_r} \sum_{h=\max(j,k)}^{n_r} \text{trace} \left[\frac{\partial \mathbf{T}_h}{\partial q_{v,i}} \mathbf{J}_h \frac{\partial^2 \mathbf{T}_h^T}{\partial q_{r,j} \partial q_{r,k}} \right] \dot{q}_{r,j} \dot{q}_{r,k}$$

$$R_v(i, j) = \sum_{k=j}^{n_r} \text{trace} \left[\frac{\partial \mathbf{T}_k}{\partial q_{v,i}} \mathbf{J}_k \frac{\partial \mathbf{T}_k^T}{\partial q_{r,j}} \right] \quad 1 \leq i \leq n_v, 1 \leq j \leq n_r$$

Τέλος, αναφέρεται ότι ο πίνακας \mathbf{R}_v πρέπει να είναι ανάστροφος του \mathbf{R}_r , διότι αναφέρονται στις δυνάμεις αλληλεπίδρασης μεταξύ Πλατφόρμας και Χειριστή. Αυτοί οι πίνακες, μαζί με τα αντίστοιχα μητρώα μάζας των εξισώσεων των υποσυστημάτων θα αποτελέσουν, τελικά, το συνολικό μητρώο του συστήματος που θα πρέπει να είναι θετικά ορισμένος πίνακας. Αυτό μπορεί να επιβεβαιωθεί εξετάζοντας τις εξισώσεις ορισμού των εν λόγω πινάκων. Λαμβάνοντας υπόψη τα παραπάνω, οι επαυξημένες δυναμικές εξισώσεις της Πλατφόρμας

$$\mathbf{M}_{v1}\ddot{\mathbf{q}}_v + \mathbf{C}_{v1}(\mathbf{q}_v, \dot{\mathbf{q}}_v) + \mathbf{C}_{v2}(\mathbf{q}_v, \mathbf{q}_r, \dot{\mathbf{q}}_v, \dot{\mathbf{q}}_r) = \boldsymbol{\tau}_v - \mathbf{D}_v - \mathbf{M}_{v2}(\mathbf{q}_v, \mathbf{q}_r)\ddot{\mathbf{q}}_v - \mathbf{R}_v(\mathbf{q}_v, \mathbf{q}_r)\ddot{\mathbf{q}}_v$$

και του Χειριστή

$$\mathbf{M}_{r1}(\mathbf{q}_r)\ddot{\mathbf{q}}_r + \mathbf{C}_{r1}(\mathbf{q}_r, \dot{\mathbf{q}}_r) + \mathbf{C}_{r2}(\mathbf{q}_r, \dot{\mathbf{q}}_r, \dot{\mathbf{q}}_v) + \mathbf{G}_r(\mathbf{q}_r) + \mathbf{D}_r\dot{\mathbf{q}}_r = \boldsymbol{\tau}_r - \mathbf{R}_r(\mathbf{q}_v, \mathbf{q}_r)\ddot{\mathbf{q}}_v$$

Προς συντόμευση των εξισώσεων παραλείπονται τα ορίσματα καθώς και γράφονται σε μητρωϊκή γραφή

$$\begin{bmatrix} \mathbf{M}_v & \mathbf{R}_v \\ \mathbf{R}_r & \mathbf{M}_r \end{bmatrix} \begin{bmatrix} \ddot{\mathbf{q}}_v \\ \ddot{\mathbf{q}}_r \end{bmatrix} + \begin{bmatrix} \mathbf{C}_v \\ \mathbf{C}_r \end{bmatrix} + \begin{bmatrix} \mathbf{0}_{n_v} \\ \mathbf{G}_r \end{bmatrix} + \begin{bmatrix} \mathbf{D}_v \\ \mathbf{D}_r\dot{\mathbf{q}}_r \end{bmatrix} = \begin{bmatrix} \boldsymbol{\tau}_v \\ \boldsymbol{\tau}_r \end{bmatrix}$$

όπου

$$\begin{aligned} \mathbf{M}_v &= \mathbf{M}_{v1} + \mathbf{M}_{v2} \\ \mathbf{C}_v &= \mathbf{C}_{v1} + \mathbf{C}_{v2} \\ \mathbf{M}_r &= \mathbf{M}_{r1} \\ \mathbf{C}_r &= \mathbf{C}_{r1} + \mathbf{C}_{r2} \end{aligned}$$

και επιπλέον

$$\begin{bmatrix} \boldsymbol{\tau}_v \\ \boldsymbol{\tau}_r \end{bmatrix} = \begin{bmatrix} \mathbf{E}_v \boldsymbol{\tau}_w \\ \boldsymbol{\tau}_r \end{bmatrix} = \begin{bmatrix} \mathbf{E}_v & \mathbf{0}_{n_v \times n_r} \\ \mathbf{0}_{n_r \times n_w} & \mathbf{I}_{n_r \times n_r} \end{bmatrix} \begin{bmatrix} \boldsymbol{\tau}_w \\ \boldsymbol{\tau}_r \end{bmatrix}$$

Οι δυναμικές εξισώσεις μπορούν να συντομευθούν περαιτέρω στη τυπική μορφή των δυναμικών εξισώσεων Χειριστών

$$\mathbf{M}\ddot{\mathbf{q}} + \mathbf{C} + \mathbf{G} + \mathbf{D} = \mathbf{E}\boldsymbol{\tau}$$

όπου τα μητρώα

$$\begin{aligned} \mathbf{M} &= \begin{bmatrix} \mathbf{M}_v & \mathbf{R}_v \\ \mathbf{R}_r & \mathbf{M}_r \end{bmatrix} \in \mathbb{R}^{n \times n}, & \mathbf{C} &= \begin{bmatrix} \mathbf{C}_v \\ \mathbf{C}_r \end{bmatrix} \in \mathbb{R}^n \\ \mathbf{G} &= \begin{bmatrix} \mathbf{0}_{n_v} \\ \mathbf{G}_r \end{bmatrix} \in \mathbb{R}^n, & \mathbf{D} &= \begin{bmatrix} \mathbf{D}_v \\ \mathbf{D}_r\dot{\mathbf{q}}_r \end{bmatrix} \in \mathbb{R}^n, & \mathbf{E} &= \begin{bmatrix} \mathbf{E}_v & \mathbf{0}_{n_v \times n_r} \\ \mathbf{0}_{n_r \times n_w} & \mathbf{I}_{n_r \times n_r} \end{bmatrix} \in \mathbb{R}^{n \times (n_w + n_r)} \end{aligned}$$

και τα διανύσματα

$$\mathbf{q} = \begin{bmatrix} \mathbf{q}_v \\ \mathbf{q}_r \end{bmatrix} \in \mathbb{R}^n, \quad \boldsymbol{\tau} = \begin{bmatrix} \boldsymbol{\tau}_w \\ \boldsymbol{\tau}_r \end{bmatrix} \in \mathbb{R}^{n_w + n_r}$$

όπου $n = n_v + n_r$ είναι οι συνολικοί βαθμοί ελευθερίας του Κινητού Χειριστή, n_r του Χειριστή, n_v της Πλατφόρμας και n_w οι φαινόμενοι είσοδοι της Πλατφόρμας, που ουσιαστικά είναι το πλήθος των ροδών.

Τέλος, όταν ο Κινητός Χειριστής αλληλεπιδρά με το περιβάλλον, αναπτύσσονται δυνάμεις $\mathbf{f}_e \in \mathbb{R}^{3 \times 1}$, και ροπές, $\boldsymbol{\mu}_e \in \mathbb{R}^{3 \times 1}$. Μπορούν να παρασταθούν μαζί, στο διάνυσμα δυναμο-ροπής

$$\mathbf{h}_e = \begin{bmatrix} \mathbf{f}_e \\ \boldsymbol{\mu}_e \end{bmatrix} \in \mathbb{R}^{6 \times 1}$$

και οι δυναμικές εξισώσεις γράφονται

$$\mathbf{M}\ddot{\mathbf{q}} + \mathbf{n} = \mathbf{E}\boldsymbol{\tau} + \mathbf{J}^T \mathbf{h}_e$$

όπου όλοι οι όροι εκτός της επιτάχυνσης έχουν ομαδοποιηθεί $\mathbf{n}(\mathbf{q}, \dot{\mathbf{q}}) = \mathbf{n} = \mathbf{C} + \mathbf{G} + \mathbf{D}$ για να διευκολυνθεί η ανάλυση στην επόμενη ενότητα. Οι δυναμικές εξισώσεις μπορούν, επίσης, να γραφούν στο πεδίο δράσης, ήτοι ως προς τον ακροδέκτη. Δια αισθητικά, μια τέτοια ανάλυση είναι δικαιολογημένη καθώς η δυναμική του ακροδέκτη έχει σημαίνοντα ρόλο στην δυναμική του αντικειμένου, με το οποίο συνδέεται, και το οποίο θέλουμε να ελέγξουμε. Η μορφή της εξίσωσης είναι ανάλογη με εκείνη στο χώρο αρθρώσεων

$$\tilde{\mathbf{M}}\dot{\mathbf{v}}_e + \tilde{\mathbf{C}} + \tilde{\mathbf{G}} + \tilde{\mathbf{D}} = \mathbf{u} + \mathbf{h}_e$$

Βασική σχέση για να πραγματοποιηθεί η αλλαγή του χώρου παράστασης της δυναμικής είναι η σχέση της Διαφορικής Κινηματικής που αν παραγωγιστεί δίνει

$$\dot{\mathbf{v}}_e = \ddot{\mathbf{x}}_e = \dot{\mathbf{J}}\dot{\mathbf{q}} + \mathbf{J}\ddot{\mathbf{q}}$$

Με αντικατάσταση αυτής στις δυναμικές εξισώσεις και εξ'αριστερών πολλαπλασιασμό με \mathbf{J}^{-T}

$$\mathbf{J}^{-T} \mathbf{M} \mathbf{J}^{-1} \dot{\mathbf{v}}_e + \mathbf{J}^{-T} \mathbf{M} \mathbf{J}^{-1} \dot{\mathbf{J}} \dot{\mathbf{q}} + \mathbf{J}^{-T} \mathbf{C} + \mathbf{J}^{-T} \mathbf{G} + \mathbf{J}^{-T} \mathbf{D} = \mathbf{u} + \mathbf{h}_e$$

όπου με κατάλληλη ομαδοποίηση των όρων προκύπτουν οι σχέσεις μετασχηματισμού

$$\begin{aligned} \tilde{\mathbf{M}} &= \mathbf{J}^{-T} \mathbf{M} \mathbf{J}^{-1} \\ \tilde{\mathbf{C}} &= \mathbf{J}^{-T} \mathbf{C} - \mathbf{J}^{-T} \mathbf{M} \mathbf{J}^{-1} \dot{\mathbf{J}} \dot{\mathbf{q}} \\ \tilde{\mathbf{G}} &= \mathbf{J}^{-T} \mathbf{G} \\ \tilde{\mathbf{D}} &= \mathbf{J}^{-T} \mathbf{D} \end{aligned}$$

και \mathbf{u} είναι η είσοδος στο χώρο δράσης. Τονίζεται ότι οι είσοδοι στο χώρο δράσης και στο χώρο αρθρώσεων συνδέονται με τη σχέση

$$\mathbf{E}\boldsymbol{\tau} = \mathbf{J}^T \mathbf{u}$$

Επίσης, σε περίπτωση που έχει επιλεγθεί κάποια ελαχιστοτική αναπαράσταση για τον προσανατολισμό, η παραπάνω διαδικασία μπορεί να επαναληφθεί έτσι ώστε οι εξισώσεις να εκφραστούν με ένα άλλο γενικευμένο διάνυσμα ταχυτήτων. Σε αυτή τη περίπτωση τη θέση της Ιακωβιανής λαμβάνει ο αντίστροφος του πίνακα \mathbf{T}_A που αναφέρθηκε στην

Διαφορική Κινηματική ανάλυση. Ακόμα, τα παραπάνω ισχύουν για τη περίπτωση του μη-πλεοναστού Χειριστή. Επειδή οι Κινητοί Χειριστές είναι εν γένει πλεοναστοί πρέπει να γίνουν κάποιες προσθήκες και διαφοροποιήσεις στις σχέσεις αυτές. Αρχικά στη σχέση μεταξύ των εισόδων θα πρέπει να ληφθεί

$$\mathbf{E}\boldsymbol{\tau} = \mathbf{J}^T \mathbf{u} + [\mathbf{I} - \mathbf{J}^T \mathbf{J}^{T\#}] \boldsymbol{\tau}_o$$

όπου $\boldsymbol{\tau}_o$ είναι ένα γενικευμένο διάνυσμα ροπών, το οποίο προβάλλεται στον ορθογώνιο υπόχωρο του γενικευμένου αντίστροφου $\mathbf{J}^{T\#}$ και οι μετασχηματισμένοι πίνακες

$$\tilde{\mathbf{M}} = (\mathbf{J}\mathbf{M}^{-1}\mathbf{J}^T)^{-1}$$

$$\tilde{\mathbf{C}} = \bar{\mathbf{J}}^T \mathbf{C} - \tilde{\mathbf{M}}\dot{\bar{\mathbf{J}}}$$

$$\tilde{\mathbf{G}} = \bar{\mathbf{J}}^T \mathbf{G}$$

$$\tilde{\mathbf{D}} = \bar{\mathbf{J}}^T \mathbf{D}$$

Επειδή η Ιακωβιανή δεν είναι τετράγωνη, λόγω της πλεοναστότητας, θα χρειαζόταν η εύρεση ενός ψευδο-αντίστροφου. Με σκοπό να αποφευχθεί, σε πρώτο στάδιο, ο υπολογισμός του αντίστροφου της Ιακωβιανής, το μητρώο αδράνειας υπολογίζεται με αυτό το τρόπο. Επίσης στις παραπάνω σχέσεις εμφανίζεται ο *δυναμικά συνεπής* [32] ψευδο-αντίστροφος της Ιακωβιανής

$$\bar{\mathbf{J}}^T = \mathbf{J}^{T\#} = \tilde{\mathbf{M}}\mathbf{J}\mathbf{M}^{-1}$$

που είναι εκείνος ο ψευδο-αντίστροφος για τον οποίο η εσωτερική φόρτιση στο χώρο δράσης, που εκφράζεται από τον όρο με το διάνυσμα $\boldsymbol{\tau}_o$, δεν παράγει κίνηση στον αχροδέκτη.

Μοντελοποίηση Αντικειμένου

Σχετικά με το αντικείμενο προς μεταφορά, επιλέγεται μία βασική μοντελοποίηση που περιλαμβάνει μόνο την αδράνεια του αντικειμένου. Για τις μικρές ταχύτητες μεταφοράς που μελετάται αυτή η θεώρηση είναι αρκετά ακριβής. Η θέση και ο προσανατολισμός του k-στού αχροδέκτη που πιάνει στερεά το αντικείμενο, βάση της σύμβασης "virtual stick" εκφράζεται ως

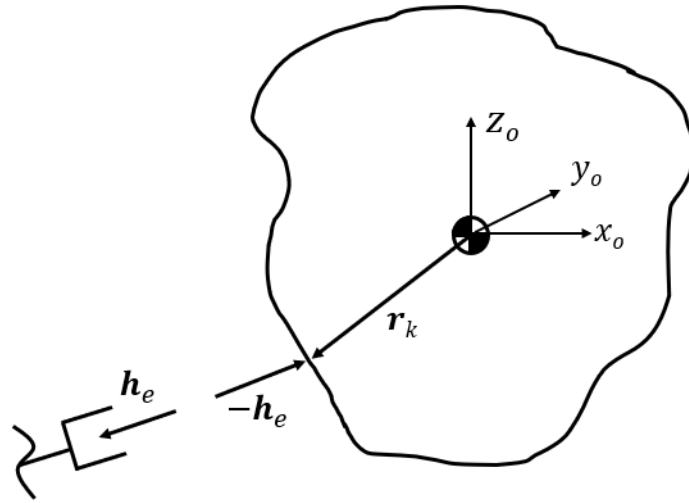
$$\mathbf{p}_k = \mathbf{p}_o + \mathbf{r}_k^o$$

$$\mathbf{R}_k = \mathbf{R}_o {}^o\mathbf{R}_k$$

όπου \mathbf{r}_k^o είναι το διάνυσμα από το Σύστημα Συντεταγμένων στο κέντρο μάζας του αντικειμένου προς τον αχροδέκτη εκπεφρασμένο στο αδρανειακό Σύστημα Συντεταγμένων και ${}^o\mathbf{R}_k$ παριστάνει τον σχετικό προσανατολισμό. Έπειτα, ο αχροδέκτης και το αντικείμενο μπορούν να χαρακτηριστούν, ως προς την αλληλεπίδραση τους, με τη θέση αρπαγής και τη σχετική Ιακωβιανή του αντικειμένου. Σύμφωνα με τον νόμο ταχυτήτων

$$\mathbf{v}_k = \mathbf{v}_o + \boldsymbol{\omega}_o \times {}^o\mathbf{r}_k^o$$

$$\boldsymbol{\omega}_k = \boldsymbol{\omega}_o$$



Σχήμα 2: Διάγραμμα Ελευθέρου Σώματος της αλληλεπίδρασης μεταξύ ακροδέκτη και αντικειμένου

όπου ${}^o r_k^o$ ταυτίζεται με το r_k στο σχήμα 2. Οι σχέσεις αυτές σε μητρική γραφή είναι

$$v_k = J_{ok} v_o = \begin{bmatrix} \mathbf{I}_{3 \times 3} & -[r_k]_{\times} \\ \mathbf{0}_{3 \times 3} & \mathbf{I}_{3 \times 3} \end{bmatrix} v_o$$

όπου $\mathbf{S}(\cdot)$ είναι ο αντι-συμμετρικός τελεστής. Τέλος, η Ιακωβιανή είναι πάντα πλήρους βαθμού λόγω της στερεής σύνδεσης.

Οι γενικευμένες συντεταγμένες του αντικειμένου ορίζονται με το διάνυσμα

$$x_o = \begin{bmatrix} p_o \\ \varphi_o \end{bmatrix} \in \mathbb{R}^{6 \times 1}$$

που εκφράζει τη θέση και τον προσανατολισμό του αντικειμένου, λ.χ. υιοθετώντας κάποιο ελαχιστοτικό προσανατολισμό όπως οι γωνίες Euler ZYX. Αντίστοιχα, οι γενικευμένες ταχύτητες

$$v_o = \begin{bmatrix} \dot{p}_o \\ \omega_o \end{bmatrix} \in \mathbb{R}^{6 \times 1}$$

Το αντικείμενο θεωρείται στερεό και ως εκ τούτου ισχύουν οι δυναμικές εξισώσεις στερεού αντικειμένου

$$\mathbf{M}_o \dot{v}_o + \mathbf{C}_o(v_o) v_o + \mathbf{G}_o + \mathbf{D}_o = \mathbf{h}_o$$

ή αλλιώς κατ' αναλογία της συντόμευσης στις εξισώσεις του Χειριστή

$$\mathbf{M}_o \dot{v}_o + \mathbf{n}_o = \mathbf{h}_o$$

όπου

$$\mathbf{M}_o = \begin{bmatrix} m_o \mathbf{I}_{3 \times 3} & \mathbf{0} \\ \mathbf{0} & \mathbf{I}_o \end{bmatrix}$$

$$\mathbf{C}_o = \begin{bmatrix} m_o [\boldsymbol{\omega}_o]_{\times} & \mathbf{0}_{3 \times 3} \\ \mathbf{0}_{3 \times 3} & [\boldsymbol{\omega}_o]_{\times} \mathbf{I}_o \end{bmatrix}$$

$$\mathbf{G}_o = \begin{bmatrix} m_o \mathbf{g} \\ \mathbf{0} \end{bmatrix}$$

όπου \mathbf{D}_o εκφράζει τη τριβή, m_o η μάζα και \mathbf{I}_o ο τανυστής αδράνειας του αντικειμένου. Το μητρώο Coriolis, \mathbf{C}_o παρουσιάζεται για λόγους πληρότητας αν και στην εφαρμογή δε λαμβάνεται υπόψη. Τέλος, \mathbf{h}_o είναι η συνολική δυναμο-ροπή που ασκεί ο ακροδέκτης στο αντικείμενο

$$\mathbf{h}_o = -\mathbf{G}\mathbf{h}_e \quad (1)$$

όπου $\mathbf{G} = \mathbf{G}_k = \mathbf{J}_{o_k}^T$ είναι το μητρώο αρπαγής που συσχετίζει τη δυναμο-ροπή στον εκάστοτε ακροδέκτη με τη δυναμο-ροπή όπως την αντιλαμβάνεται το κέντρο μάζας του αντικειμένου. Τονίζεται η μορφή αυτή ισχύει για την επίπεδη θεώρηση ενώ για τις άλλες περιπτώσεις το μητρώο πρέπει να τροποποιηθεί κατάλληλα ώστε να ληφθεί υπόψη ο μετασχηματισμός που συσχετίζει τη γωνιακή ταχύτητα με την παράγωγο του προσανατολισμού [37]

$$\mathbf{G}_k = \begin{bmatrix} \mathbf{I}_{3 \times 3} & \mathbf{0}_{3 \times 3} \\ \mathbf{T}_A^T \mathbf{S}(\mathbf{r}_k) & \mathbf{T}_A^T \end{bmatrix}$$

Υπολογισμός Δυναμο-Ροπής Αλληλεπίδρασης

Η πραγματοποίηση των προσομοιώσεων ενός τέτοιου συστήματος επιβάλλει τη γνώση των δυνάμεων αλληλεπίδρασης μεταξύ ρομπότ και αντικειμένων. Αρχικά, θεωρούνται οι περιορισμοί οι οποίοι συνεπάγονται της στερεής αρπαγής του αντικειμένου και εκφράζονται μαθηματικά από τη σχέση

$$\mathbf{x}_o = \mathbf{H}(\mathbf{q})$$

Δηλαδή η πόζα του αντικειμένου καθορίζεται από τη πόζα του εκάστοτε ρομπότ. Για να βρεθεί η έκφραση του περιορισμού θεωρείται ο ομογενής μετασχηματισμός μεταξύ αντικειμένου και ρομπότ, από την οπτική του αντικειμένου, ως η πλέον κατάλληλη για τη διαισθητική αντίληψη του.

$${}^o\mathbf{T}_e = \begin{bmatrix} {}^o\mathbf{R}_e & {}^o\mathbf{p}_e \\ \mathbf{0}_{3 \times 1} & 1 \end{bmatrix}$$

Όμως για να συνδεθεί με τη κινηματική ανάλυση που έχει προηγηθεί, πρέπει ο μετασχηματισμός να εκφραστεί ως προς τον ακροδέκτη

$${}^e\mathbf{T}_o = \begin{bmatrix} {}^o\mathbf{R}_e^T & -{}^o\mathbf{R}_e^T {}^o\mathbf{p}_e \\ \mathbf{0}_{3 \times 1} & 1 \end{bmatrix}$$

Ο σχετικός προσανατολισμός μπορεί να οριστεί με την υιοθέτηση γωνιών Euler ή κάποιας άλλης αναπαράστασης προσανατολισμού. Τέλος η αναγκαία περιγραφή της πόζας του αντικειμένου προκύπτει

$${}^W\mathbf{T}_o = {}^W\mathbf{T}_e = {}^W\mathbf{T}_V \cdot {}^V\mathbf{T}_M \cdot {}^M\mathbf{T}_e \cdot {}^e\mathbf{T}_o = \begin{bmatrix} \mathbf{R}_o & \mathbf{p}_o \\ \mathbf{0}_{1 \times 3} & 1 \end{bmatrix}$$

Το σύστημα των διαφορικών εξισώσεων ρομποτ και αντικειμένου μαζί με τους περιορισμούς αποτελεί ένα αλγεβρικό-διαφορικό σύστημα. Εντούτοις, μπορεί να εκφραστεί ως ένα ιδιόμορφο σύστημα διαφορικών εξισώσεων [38]

$$\begin{bmatrix} \mathbf{M}(\mathbf{q}) & \mathbf{0} & \mathbf{0} \\ \mathbf{0} & \mathbf{M}_o & \mathbf{0} \\ \mathbf{0} & \mathbf{0} & \mathbf{0} \end{bmatrix} \begin{bmatrix} \ddot{\mathbf{q}} \\ \dot{\mathbf{v}}_o \\ \dot{\mathbf{h}}_e \end{bmatrix} = \begin{bmatrix} \mathbf{E}\boldsymbol{\tau} - \mathbf{n} + \mathbf{J}^T \mathbf{h}_e \\ -\mathbf{G}\mathbf{h}_e - \mathbf{n}_o \\ \mathbf{x}_o - \mathbf{H}(\mathbf{q}) \end{bmatrix}$$

Με κατάλληλη χειραγώγηση των εξισώσεων, δύναται να μετασχηματιστεί σε ένα αποκλειστικά διαφορικό σύστημα. Αρχικά θεωρείται ο αλγεβρικός περιορισμός ως

$$\mathbf{Q}(\mathbf{x}) = \mathbf{x}_o - \mathbf{H}(\mathbf{q}) = \mathbf{0}$$

όπου $\mathbf{x} = [\mathbf{q}^T \quad \mathbf{x}_o^T]^T$. Με διπλή παραγώγιση και χρήση του κανόνα της αλυσίδας

$$\frac{d\mathbf{Q}}{d\mathbf{x}} \dot{\mathbf{x}} = 0 \Rightarrow \frac{d}{dt} \left(\frac{d\mathbf{Q}}{d\mathbf{x}} \right) \dot{\mathbf{x}} + \frac{d\mathbf{Q}}{d\mathbf{x}} \ddot{\mathbf{x}} = 0$$

Ακόμα, το σύστημα δυναμικών εξισώσεων αντικειμένου και ρομπότ μπορεί να παρασταθεί με βάση το ενιαίο διάνυσμα κατάστασης, \mathbf{x} και να λυθεί ως προς την επιτάχυνση

$$\begin{bmatrix} \mathbf{M}(\mathbf{q}) & \mathbf{0} \\ \mathbf{0} & \mathbf{M}_o \end{bmatrix} \begin{bmatrix} \ddot{\mathbf{q}} \\ \ddot{\mathbf{q}}_o \end{bmatrix} = \begin{bmatrix} \mathbf{E}\boldsymbol{\tau} - \mathbf{n} + \mathbf{J}^T \mathbf{h}_e \\ -\mathbf{G}\mathbf{h}_e - \mathbf{n}_o \end{bmatrix} \Rightarrow$$

$$\mathbf{M}(\mathbf{x})\ddot{\mathbf{x}} = \mathbf{E}(\mathbf{x})\boldsymbol{\tau} - \mathbf{n}(\mathbf{x}, \dot{\mathbf{x}}) + \mathbf{B}^T(\mathbf{x})\mathbf{h}_e \Rightarrow$$

$$\ddot{\mathbf{x}} = \mathbf{M}(\mathbf{x})^{-1} [\mathbf{E}(\mathbf{x})\boldsymbol{\tau} - \mathbf{n}(\mathbf{x}, \dot{\mathbf{x}})] + \mathbf{M}(\mathbf{x})^{-1} \mathbf{B}^T(\mathbf{x})\mathbf{h}_e$$

όπου έχουν ομαδοποιηθεί στα μητρώα του σύνθετου συστήματος. Συγκεκριμένα, το μητρώο μάζας

$$\mathbf{M}(\mathbf{x}) = \begin{bmatrix} \mathbf{M}(\mathbf{q}) & \mathbf{0} \\ \mathbf{0} & \mathbf{M}_o \end{bmatrix}$$

το μητρώο Coriolis και άλλων όρων,

$$\mathbf{n}(\mathbf{x}, \dot{\mathbf{x}}) = \begin{bmatrix} \mathbf{n} \\ \mathbf{n}_o \end{bmatrix}$$

οι όροι που σχετίζονται με την επενέργηση

$$\mathbf{E}(\mathbf{x}) = \begin{bmatrix} \mathbf{E} \\ \mathbf{0} \end{bmatrix}$$

και το μητρώο που σχετίζεται με τη δυναμο-ροπή

$$\mathbf{B}(\mathbf{x}) = [\mathbf{J} \quad -\mathbf{G}^T]$$

Προς αποφυγή παρανόησης, τονίζεται ότι τα μητρώα που εμφανίζονται με ορίσματα \mathbf{x} και $\dot{\mathbf{x}}$ αναφέρονται στα μητρώα του συνδυασμένου συστήματος. Με αντικατάσταση της παραγωγισμένης εξίσωση περιορισμού στο εν λόγω σύστημα μπορεί να βρεθεί μία

έκφραση της δυναμο-ροπής αλληλεπίδρασης με την οποία μπορεί να υπολογίζεται σε κάθε βήμα της προσομοίωσης.

$$\frac{d}{dt} \left(\frac{d\mathbf{Q}}{d\mathbf{x}} \right) \dot{\mathbf{x}} + \frac{d\mathbf{Q}}{d\mathbf{x}} \mathbf{M}(\mathbf{x})^{-1} [\mathbf{E}(\mathbf{x})\boldsymbol{\tau} - \mathbf{n}(\mathbf{x}, \dot{\mathbf{x}})] + \frac{d\mathbf{Q}}{d\mathbf{x}} \mathbf{M}(\mathbf{x})^{-1} \mathbf{B}^T(\mathbf{x}) \mathbf{h}_e = 0$$

Για τη καλύτερη παρουσίαση ορίζονται οι ενδιάμεσες ποσότητες

$$\boldsymbol{\Omega} = \frac{d\mathbf{Q}}{d\mathbf{x}} \mathbf{M}^{-1}(\mathbf{x}) \mathbf{B}^T(\mathbf{x})$$

$$\boldsymbol{\Psi} = \frac{d\mathbf{Q}}{d\mathbf{x}} \mathbf{M}(\mathbf{x})^{-1} [\mathbf{n}(\mathbf{x}, \dot{\mathbf{x}}) - \mathbf{E}(\mathbf{x})\boldsymbol{\tau}] - \frac{d}{dt} \left(\frac{d\mathbf{Q}}{d\mathbf{x}} \right) \dot{\mathbf{x}}$$

η δυναμο-ροπή μπορεί να υπολογιστεί, αν $\boldsymbol{\Omega}$ είναι αντιστρέψιμος, ως

$$\mathbf{h}_e = \boldsymbol{\Omega}^{-1} \boldsymbol{\Psi}$$

Τα παραπάνω γενικεύονται για N , πλήθος ρομποτ που συνεργάζονται.

Σχήμα Ελέγχου

Επειδή το περιβάλλον συμπεριφέρεται ως συμμόρφωση, είναι λογικό τα συστήματα αυτά να λειτουργούν ως εμπέδηση [39]. Ταυτόχρονα, στη βιβλιογραφία υπάρχουν πολλές περιπτώσεις επιτυχούς χρήσης συστημάτων ελέγχου που βασίζονται στη χρήση Ελέγχου Εμπέδησης. Ίδια πορεία θα ακολουθηθεί και στη παρούσα εργασία. Η επιθυμητή συμπεριφορά εμπέδησης επιλέγεται ως

$$\mathbf{M}_{des} \ddot{\mathbf{e}} + \mathbf{K}_d \dot{\mathbf{e}} + \mathbf{K}_p \mathbf{e} = \mathbf{h}_{o,env}$$

όπου $\mathbf{e} = \mathbf{x}_{des} - \mathbf{x}_o$ και αντίστοιχα για τις παραγώγους. \mathbf{M}_{des} , \mathbf{K}_d , \mathbf{K}_p διαγώνιοι πίνακες κερδών, κατάλληλου μεγέθους. Η επιθυμητή είσοδος για κάθε ακροδέκτη, δηλαδή η επιθυμητή δυναμο-ροπή που θα ασκεί στο αντικείμενο χωρίζεται ως εξής

$$\mathbf{u}_i = \mathbf{u}_{m,i} + \mathbf{u}_{f,i}$$

όπου $\mathbf{u}_{m,i}$ είναι η συνεισφορά σχετικά με τη κίνηση του ακροδέκτη και $\mathbf{u}_{f,i}$ σχετίζεται με τη δύναμη που πρέπει να ασκηθεί στο αντικείμενο. Από τη δυναμική του αντικειμένου

$$\hat{\mathbf{G}} \hat{\mathbf{h}}_e = \mathbf{M}_o \mathbf{M}_{des}^{-1} [\mathbf{M}_{des} \ddot{\mathbf{x}}_{o,des} + \mathbf{K}_d \dot{\mathbf{e}} + \mathbf{K}_p \mathbf{e} - \mathbf{h}_{o,env}] + \mathbf{n}_o$$

Με αυτή τη σχέση, διαφαίνεται η γραμμικοποίηση του συστήματος μέσω ανάδρασης και μέσω του ψευδο-αντίστροφου του πίνακα αρπαγής η συνεισφορά δύναμης κάθε ρομπότ για τη κίνηση του αντικειμένου βρίσκεται

$$\mathbf{u}_f = \hat{\mathbf{G}}^\# \hat{\mathbf{G}} \hat{\mathbf{h}}_e + (\mathbf{I} - \hat{\mathbf{G}}^\# \hat{\mathbf{G}}) \mathbf{h}_I$$

όπου $\mathbf{u}_f = [\mathbf{u}_{f,1}^T \quad \mathbf{u}_{f,2}^T \quad \dots \quad \mathbf{u}_{f,N}^T]^T$ και \mathbf{h}_I είναι οι εσωτερικές δυνάμεις που ασκούνται στο αντικείμενο. Η ίδια σχέση εμπέδησης εφαρμόζεται και στους ακροδέκτες

$$\mathbf{u}_{m,i} = \tilde{\mathbf{M}} \mathbf{M}_{des}^{-1} [\mathbf{M}_{des} \ddot{\mathbf{x}}_{des,i} + \mathbf{K}_d \dot{\mathbf{e}}_i + \mathbf{K}_p \mathbf{e}_i - \mathbf{h}_{I,i}] + \tilde{\mathbf{n}}$$

όπου το σφάλμα ορίζεται αντίστοιχα και \mathbf{h}_I^i η συνεισφορά του i -στου ακροδέκτη στην εσωτερική δύναμη που αναπτύσσεται [36]. Τέλος, αναφέρεται ότι καλύτερα αποτελέσματα του σχήματος ελέγχου παρατηρούνται όταν τα κέρδη της επιθυμητής εμπέδησης είναι κοινά [37].

Προσομοίωση και Αποτελέσματα

Η κινηματική και δυναμική μελέτη του συστήματος, ήτοι η παραγωγή των κατάλληλων μητρώων πραγματοποιήθηκε με χρήση του λογισμικού MATLAB[®] και συγκεκριμένα με το Symbolic Toolbox. Η προσομοίωση του συστήματος πραγματοποιήθηκε με το Simulink[®]. Δοκιμάστηκε ένα απλό σύστημα. Αποτελείται από δύο Κινητούς Χειριστές που διαθέτουν Χειριστή με έναν βαθμό ελευθερίας. Επομένως και το αντικείμενο και ο ακροδέκτης πραγματοποιούν επίπεδη κίνηση. Η δοκιμή είναι απλή μεταφορά αντικειμένου χωρίς απαίτηση εσωτερικής φόρτισης. Για τις υπολογισθείσες τιμές της δυναμο-ροπής αλληλεπίδρασης θεωρείται 5% απόκλιση από την ονομαστική τιμή και 10ms καθυστέρηση στην απόδοση της τιμής. Το αντικείμενο θεωρήθηκε ότι είναι ορθογωνικό και έχει μάζα $m_0 = 100kg$ και ροπή αδράνειας $I_0 = 4.3kgm^2$. Η επιθυμητή τροχιά λειτουργεί ως αναφορά για τον ελεγκτή και τα κέρδη επιλέχθηκαν ως

$$\mathbf{M}_{des} = 100\mathbf{I}_{3 \times 3}$$

$$\mathbf{K}_d = 800\mathbf{I}_{3 \times 3}$$

$$\mathbf{K}_p = 600\mathbf{I}_{3 \times 3}$$

Δοκιμάζονται η κυκλική και ημιτονοειδής τροχιά κίνησης. Μάλιστα για τη πρώτη περίπτωση γίνεται περαιτέρω δοκιμή με την ύπαρξη της στατικής τριβής μεταξύ αντικειμένου και επιπέδου κίνησης. Η απουσία τριβής μπορεί να αντιστοιχισθεί στη περίπτωση που το αντικείμενο που μεταφέρεται είναι στον αέρα. Ο ελεγκτής παράγει καλά αποτελέσματα και γίνεται επαρκής παρακολούθηση της τροχιάς. Ένα μικρό σφάλμα παραμένει μετά το τέλος της τροχιάς που οφείλεται στην απουσία ολοκληρωτικής δράσης του ελεγκτή. Οι παραπάνω δοκιμές επιβεβαιώνουν την ορθή λειτουργία του δυναμικού μοντέλου, καθώς και την αποτελεσματικότητα του σχήματος ελέγχου. Τούτο είναι σημαντικό διότι το εν λόγω μοντέλο αποτελεί τη βάση για μία πληθώρα ερευνητικών ενδιαφερόντων, όπως η ανάπτυξη λογισμικού για αυτόνομη λειτουργία τέτοιων Χειριστών με Τεχνητή Νοημοσύνη και αλγορίθμων για την αποδοτική και ασφαλή συνεργασία ρομπότ και ανθρώπων. Αμφότερα αποτελούν ερευνητικά πεδία υψηλού ενδιαφέροντος που μπορούν να βελτιώσουν την παραγωγικότητα και να αναλάβουν επικίνδυνες ή δύσκολες εργασίες.

Bibliography

- [1] R. Paul, “Robots, models, and automation,” *Computer*, vol. 12, no. 7, pp. 19–27, 1979.
- [2] E. Freund and M. Syrbe, “Control of industrial robots by means of microprocessors,” 1977.
- [3] R. P. Kruger and W. B. Thompson, “A technical and economic assessment of computer vision for industrial inspection and robotic assembly,” *Proceedings of the IEEE*, vol. 69, pp. 1524–1538, 1981.
- [4] Y. Shirai and H. Inoue, “Guiding a robot by visual feedback in assembling tasks,” *Pattern Recognition*, vol. 5, no. 2, pp. 99–106, IN3,107–108, 1973.
- [5] A. Johnston, “Optical proximity sensors for manipulators,” Jet Propulsion Laboratory, California Institute of Technology, Tech. Rep., 1973.
- [6] M. Ueda, K. Iwata, T. Shimizu, and I. Sakai, “Sensors and systems of an industrial robot,” *Memoirs of the School of Engineering, Nagoya University*, vol. 27, no. 2, pp. 163–207, 1975.
- [7] D. Cahn and S. Phillips, “Robnav: A range-based robot navigation and obstacle avoidance algorithm,” *IEEE Transactions on Systems, Man and Cybernetics*, vol. SMC-5, no. 5, pp. 544–551, 1975.
- [8] A. Flynn, “Combining sonar and infrared sensors for mobile robot navigation,” *The International Journal of Robotics Research*, vol. 7, no. 6, pp. 5–14, 1988.
- [9] M. S. Bahraini, A. B. Rad, and M. Bozorg, “Slam in dynamic environments: A deep learning approach for moving object tracking using ml-ransac algorithm,” *Sensors*, vol. 19, no. 17, 2019. [Online]. Available: <https://www.mdpi.com/1424-8220/19/17/3699>
- [10] M. Raibert and J. Craig, “Hybrid position/force control of manipulators,” *Journal of Dynamic Systems, Measurement and Control, Transactions of the ASME*, vol. 103, no. 2, pp. 126–133, 1981.
- [11] G. Saridis, “Toward the realization of intelligent controls,” *Proceedings of the IEEE*, vol. 67, no. 8, pp. 1115–1133, 1979.
- [12] K. Fu, “Learning control systems and intelligent control systems: An intersection of artificial intelligence and automatic control,” *IEEE Transactions on Automatic Control*, vol. 16, no. 1, pp. 70–72, 1971.
- [13] M. Boden, “Impacts of artificial intelligence,” *Futures*, vol. 16, no. 1, pp. 60–70, 1984.
- [14] M. Brady, “Artificial intelligence and robotics,” *Artificial Intelligence*, vol. 26, no. 1, pp. 79–121, 1985.

- [15] K. I. Alevizos, C. P. Bechlioulis, and K. J. Kyriakopoulos, “Physical human–robot cooperation based on robust motion intention estimation,” *Robotica*, vol. 38, no. 10, p. 1842–1866, 2020.
- [16] A. Mörtl, M. Lawitzky, A. Kucukyilmaz, M. Sezgin, C. Basdogan, and S. Hirche, “The role of roles: Physical cooperation between humans and robots,” *The International Journal of Robotics Research*, vol. 31, no. 13, pp. 1656–1674, 2012.
- [17] V. Moysiadis, N. Tsolakis, D. Katikaridis, C. Sørensen, S. Pearson, and D. Bochtis, “Mobile robotics in agricultural operations: A narrative review on planning aspects,” *Applied Sciences (Switzerland)*, vol. 10, no. 10, 2020.
- [18] I. Kontolatis, D. Myrasiotis, I. Paraskevas, E. Papadopoulos, G. Croon, and D. Izzo, “Quadruped optimum gaits analysis for planetary exploration,” 05 2013.
- [19] M. Tranzatto, F. Mascarich, L. Bernreiter, C. Godinho, M. Camurri, S. Khat-tak, T. Dang, V. Reijgwart, J. Loeje, D. Wisth, S. Zimmermann, H. Nguyen, M. Fehr, L. Solanka, R. Buchanan, M. Bjelonic, N. Khedekar, M. Valceschini, F. Jenelten, M. Dharmadhikari, T. Homberger, P. D. Petris, L. Wellhausen, M. Kulkarni, T. Miki, S. Hirsch, M. Montenegro, C. Papachristos, F. Tresoldi, J. Carius, G. Valsecchi, J. Lee, K. Meyer, X. Wu, J. Nieto, A. Smith, M. Hutter, R. Siegwart, M. Mueller, M. Fallon, and K. Alexis, “Cerberus: Autonomous legged and aerial robotic exploration in the tunnel and urban circuits of the darpa subterranean challenge,” 2022.
- [20] M. Dorigo, V. Maniezzo, and A. Coloni, “Ant system: Optimization by a colony of cooperating agents,” *IEEE Transactions on Systems, Man, and Cybernetics, Part B: Cybernetics*, vol. 26, no. 1, pp. 29–41, 1996, cited By 8894.
- [21] M. Dorigo and L. Gambardella, “Ant colony system: A cooperative learning approach to the traveling salesman problem,” *IEEE Transactions on Evolutionary Computation*, vol. 1, no. 1, pp. 53–66, 1997, cited By 6118. [Online]. Available: <https://www.scopus.com/inward/record.uri?eid=2-s2.0-0031122887&doi=10.1109%2F4235.585892&partnerID=40&md5=55a90df80907d00464d7a696500d935b>
- [22] M. Dorigo, M. Birattari, and T. Stützle, “Ant colony optimization artificial ants as a computational intelligence technique,” *IEEE Computational Intelligence Magazine*, vol. 1, no. 4, pp. 28–39, 2006, cited By 2829. [Online]. Available: <https://www.scopus.com/inward/record.uri?eid=2-s2.0-33846280533&doi=10.1109%2Fci-m.2006.248054&partnerID=40&md5=d3cc744b99f9da911ff4d1776cb75e40>
- [23] Y. Hirata and K. Kosuge, “Distributed robot helpers handling a single object in cooperation with a human,” in *Proceedings 2000 ICRA. Millennium Conference. IEEE International Conference on Robotics and Automation. Symposia Proceedings (Cat. No.00CH37065)*, vol. 1, 2000, pp. 458–463 vol.1.

- [24] B. Siciliano, L. Sciavicco, V. Luigi, and G. Oriolo, *Robotics: Modelling, planning and control*, 01 2009.
- [25] N. A. Hootsmans, “The motion control of manipulators on mobile vehicles,” PhD Dissertation, 1992.
- [26] E. Papadopoulos, *Robotics Notes - National Technical University of Athens (NTUA)*, 2021.
- [27] K. Zimmermann, I. Zeidis, and M. Abdelrahman, “Dynamics of mechanical systems with mecanum wheels,” vol. 93, pp. 269–279, 01 2014.
- [28] Y. Yamamoto, “Control and coordination of locomotion and manipulation of a wheeled mobile manipulators,” PhD Dissertation, 1994.
- [29] S. Tzafestas, *Introduction to Mobile Robot Control*, 2014.
- [30] N. Tlale and M. de Villiers, “Kinematics and dynamics modelling of a mecanum wheeled mobile platform,” in *2008 15th International Conference on Mechatronics and Machine Vision in Practice*, 2008, pp. 657–662.
- [31] R. Jazar, *Theory of applied robotics: Kinematics, dynamics, and control (2nd Edition)*, 2010.
- [32] O. Khatib, “Inertial properties in robotic manipulation: An object-level framework,” *The International Journal of Robotics Research*, vol. 14, no. 1, pp. 19–36, 1995.
- [33] G. Montemayor and J. Wen, “Decentralized collaborative load transport by multiple robots,” in *Proceedings of the 2005 IEEE International Conference on Robotics and Automation*, 2005, pp. 372–377.
- [34] Z. Wang and M. Schwager, *Multi-robot Manipulation Without Communication*, 01 2016, pp. 135–149.
- [35] S. Schneider and R. Cannon, “Object impedance control for cooperative manipulation: theory and experimental results,” *IEEE Transactions on Robotics and Automation*, vol. 8, no. 3, pp. 383–394, 1992.
- [36] B. Siciliano and O. Khatib, *Springer Handbook of Robotics*. Berlin, Heidelberg: Springer-Verlag, 2007.
- [37] S. Moosavian and E. Papadopoulos, “Multiple impedance control for object manipulation,” in *Proceedings. 1998 IEEE/RSJ International Conference on Intelligent Robots and Systems. Innovations in Theory, Practice and Applications (Cat. No.98CH36190)*, vol. 1, 1998, pp. 461–466 vol.1.
- [38] N. McClamroch, “Singular systems of differential equations as dynamic models for constrained robot systems,” in *Proceedings. 1986 IEEE International Conference on Robotics and Automation*, vol. 3, 1986, pp. 21–28.

- [39] N. Hogan, “Impedance control: An approach to manipulation,” in *1984 American Control Conference*, 1984, pp. 304–313.
- [40] P. Hsu and S. Su, “Coordinated control of multiple manipulator systems-experimental results,” in *Proceedings 1992 IEEE International Conference on Robotics and Automation*, 1992, pp. 2199–2204 vol.3.
- [41] S. Erhart, D. Sieber, and S. Hirche, “An impedance-based control architecture for multi-robot cooperative dual-arm mobile manipulation,” in *2013 IEEE/RSJ International Conference on Intelligent Robots and Systems*, 2013, pp. 315–322.
- [42] A. Tsiamis, C. K. Verginis, C. P. Bechlioulis, and K. J. Kyriakopoulos, “Cooperative manipulation exploiting only implicit communication,” in *2015 IEEE/RSJ International Conference on Intelligent Robots and Systems (IROS)*, 2015, pp. 864–869.
- [43] P. Zarafshan, S. Larimi, S. Moosavian, and B. Siciliano, “Which impedance strategy is the most effective for cooperative object manipulation?” *Industrial Robot: An International Journal*, vol. 44, pp. 198–209, 03 2017.
- [44] S. A. A. Moosavian, “Dynamics and control of free-flying manipulators capturing space objects,” PhD Dissertation, 1996.
- [45] O. Khatib, “Real-time obstacle avoidance for manipulators and mobile robots,” in *Proceedings. 1985 IEEE International Conference on Robotics and Automation*, vol. 2, 1985, pp. 500–505.
- [46] E. Rimon and D. Koditschek, “Exact robot navigation using artificial potential functions,” *IEEE Transactions on Robotics and Automation*, vol. 8, no. 5, pp. 501–518, 1992.
- [47] S. Ge and Y. Cui, “New potential functions for mobile robot path planning,” *IEEE Transactions on Robotics and Automation*, vol. 16, no. 5, pp. 615–620, 2000.
- [48] P. Vadakkepat, K. C. Tan, and W. Ming-Liang, “Evolutionary artificial potential fields and their application in real time robot path planning,” in *Proceedings of the 2000 Congress on Evolutionary Computation. CEC00 (Cat. No.00TH8512)*, vol. 1, 2000, pp. 256–263 vol.1.
- [49] A. Yamashita, T. Arai, J. Ota, and H. Asama, “Motion planning of multiple mobile robots for cooperative manipulation and transportation,” *IEEE Transactions on Robotics and Automation*, vol. 19, no. 2, pp. 223–237, 2003.
- [50] T. Kalmar-Nagy, R. D’Andrea, and P. Ganguly, “Near-optimal dynamic trajectory generation and control of an omnidirectional vehicle,” *Robotics and Autonomous Systems*, vol. 46, pp. 47–64, 01 2004.

- [51] D. Bertram, J. Kuffner, R. Dillmann, and T. Asfour, “An integrated approach to inverse kinematics and path planning for redundant manipulators,” in *Proceedings 2006 IEEE International Conference on Robotics and Automation, 2006. ICRA 2006.*, 2006, pp. 1874–1879.

Appendix A Software Structure

The scripts functions used in the software implementation are listed here. A brief explanation of each script and function is given here, while more information about their usage, e.g. class of input arguments, can be found on the respective documentations.

Scripts

MobManModel.m

This script includes the parameters for the manipulator and the moving vehicle that it is attached on. For example, the masses and lengths of the manipulator links, the Denavit-Hartenberg (DH) table of the manipulator or the matrices of the dynamic model of the platform. It then uses the functions that were defined in order to calculate the matrices that correspond to the dynamic model of the Mobile Manipulator (MM). The auxiliary functions that were used are *PseudoInertia.m*, *ManKin.m*, *ManJac.m*, *MManJac.m*, *ManDyn.m*, *IntDyn.m*.

ObjAndGrasp.m

Inside this script the parameters of the object and grasp are defined. These are the inertial characteristics of the object that are expressed through the mass matrix, along with other matrices necessary such as the friction or gravity matrix. Also the grasp matrix is calculated here as it requires defining the position and orientation of the gripping, which is done with respect to the object and, consequently it is appropriate that they belong in the same script. The function *GraspMatrix.m* is used for the calculation of the Grasp Matrices.

Constraint.m

This script differentiates between the variables of each (identical) MM and proceeds to use the kinematics produced by *MobManModel.m* and the grasp condition of *ObjAndGrasp* to produce the constraint equation in symbolic form. Then, in order to carry out the differentiation with respect to time, the variables are substituted with dummy variables that are a function of time. Afterwards the original variables are substituted back. Due to the Symbolic Toolbox being used, full automation of the process was not possible.

IniConCalc.m

The script uses the constraint equations of *Constraint* to calculate the value of the states of the multiple MMs-Object system provided that the user defines *some* of the states values. For example, in the implementation carried out it was chosen that the robots platforms' lie at the Y-axis, the object lie at the X-axis and the relative orientation of the EEs and the object such that the initial condition is true for the grasp condition defined. Then the script solved the constraint equations in

order to produce the values of the position of the object along the X-axis and of the platforms along the Y-axis. All velocities were considered zero.

ControlAndFrictionParams.m

This script contains the controller gains and the friction coefficients that were implemented. A separate script was used in order to be easily accessible for changes during the calibration of the gains and the investigation of the friction effect on the closed loop system's behaviour.

Functions

PseudoInertia.m

This function calculates the Pseudo-Inertia matrix provided that the inertia tensor and mass of the body is given. Also the vector describing the position of the CoM of the body with respect to the corresponding attached frame is needed. For more information as to why this is needed, the reader is referred to the bibliography reference on the main body of the text.

ManKin.m

This function takes as input the Denavit-Hartenberg table of the manipulator and produces a cell matrix containing the successive homogeneous transformation matrices relating the End Effector position and orientation with its base.

ManJac.m

This function calculates the Jacobian of a fixed-base manipulator. To perform this calculation the arguments given are the cell matrix produced by *ManKin.m* and a character vector denoting the type of each joint, r for revolute and p for prismatic.

MManJac.m

This function takes as input the cell matrix produced by *ManKin.m* and the fixed-base Jacobian of the manipulator produced by *ManJac.m* along with the homogeneous transformation matrices relating the vehicle to the world frame and the base of the manipulator base to the vehicle frame. Then, by following the derivation of the respective section, the Jacobian of the Mobile Manipulator is calculated.

ManDyn.m

This function produces the matrices of the dynamic model of a manipulator. It can be used by itself to produce said matrices of a stand-alone, fixed-base manipulator. The arguments needed are the cell matrix produced by *ManKin.m*, the Pseudo-Inertia cell matrix produced by *PseudoInertia.m* and the symbolic variables of the generalised coordinates and velocities of the manipulator. Also the vector describing

the position of the CoM, the mass of the links, along with the gravity vector are needed in order to calculate the gravity matrix, if needed.

IntDyn.m

This functions produces the matrices that correspond to the interaction dynamics between the vehicle and the manipulator. The symbolic variables of both the vehicle and the manipulator contained in the homogeneous matrices and the Pseudo-Inertia matrix of each link are needed.

SkewSM.m

This functions takes as input a vector and produces the skew-symmetric matrix that describes the outer product.

GraspMatrix.m

This function's arguments are the position and orientation of the EEs with respect to the object and produces the grasp matrices that related the wrench vector at the gripping points with the wrenches experienced in the object's CoM. Also, optionally the matrix relating the linear and angular velocities of the object with the linear velocities and the orientation derivatives can be given in order to produce a consistent grasp matrix in the general case.